

World Journal of *Stem Cells*

World J Stem Cells 2024 February 26; 16(2): 54-227



EDITORIAL

- 54 Human dental pulp stem/stromal cells in clinical practice
Grawish ME
- 58 Multiple pretreatments can effectively improve the functionality of mesenchymal stem cells
Wan XX, Hu XM, Xiong K
- 64 Cellular preconditioning and mesenchymal stem cell ferroptosis
Zineldeen DH, Mushtaq M, Haider KH

REVIEW

- 70 Therapeutic utility of human umbilical cord-derived mesenchymal stem cells-based approaches in pulmonary diseases: Recent advancements and prospects
Meng M, Zhang WW, Chen SF, Wang DR, Zhou CH
- 89 Unlocking the versatile potential: Adipose-derived mesenchymal stem cells in ocular surface reconstruction and oculoplastics
Surico PL, Scarabosio A, Miotti G, Grando M, Salati C, Parodi PC, Spadea L, Zeppieri M

MINIREVIEWS

- 102 Crosstalk between Wnt and bone morphogenetic protein signaling during osteogenic differentiation
Arya PN, Saranya I, Selvamurugan N
- 114 Human pluripotent stem cell-derived kidney organoids: Current progress and challenges
Long HY, Qian ZP, Lan Q, Xu YJ, Da JJ, Yu FX, Zha Y
- 126 Recent progress in hair follicle stem cell markers and their regulatory roles
Xing YZ, Guo HY, Xiang F, Li YH
- 137 Advances in the differentiation of pluripotent stem cells into vascular cells
Jiao YC, Wang YX, Liu WZ, Xu JW, Zhao YY, Yan CZ, Liu FC

ORIGINAL ARTICLE**Basic Study**

- 151 Silencing of Jumonji domain-containing 1C inhibits the osteogenic differentiation of bone marrow mesenchymal stem cells *via* nuclear factor- κ B signaling
Li JY, Wang TT, Ma L, Zhang Y, Zhu D
- 163 Effects of different concentrations of nicotinamide on hematopoietic stem cells cultured *in vitro*
Ren Y, Cui YN, Wang HW

- 176** High quality repair of osteochondral defects in rats using the extracellular matrix of antler stem cells
Wang YS, Chu WH, Zhai JJ, Wang WY, He ZM, Zhao QM, Li CY
- 191** Extracellular vesicles derived from mesenchymal stem cells mediate extracellular matrix remodeling in osteoarthritis through the transport of microRNA-29a
Yang F, Xiong WQ, Li CZ, Wu MJ, Zhang XZ, Ran CX, Li ZH, Cui Y, Liu BY, Zhao DW
- 207** VX-509 attenuates the stemness characteristics of colorectal cancer stem-like cells by regulating the epithelial-mesenchymal transition through Nodal/Smad2/3 signaling
Yuan Y, Zhang XF, Li YC, Chen HQ, Wen T, Zheng JL, Zhao ZY, Hu QY

ABOUT COVER

Editorial Board Member of *World Journal of Stem Cells*, Khawaja Husnain Haider, PhD, Professor, Department of Basic Sciences, Sulaiman Al-Rajhi University, AlQaseem 52726, Saudi Arabia. kh.haider@gmail.com

AIMS AND SCOPE

The primary aim of *World Journal of Stem Cells (WJSC, World J Stem Cells)* is to provide scholars and readers from various fields of stem cells with a platform to publish high-quality basic and clinical research articles and communicate their research findings online. *WJSC* publishes articles reporting research results obtained in the field of stem cell biology and regenerative medicine, related to the wide range of stem cells including embryonic stem cells, germline stem cells, tissue-specific stem cells, adult stem cells, mesenchymal stromal cells, induced pluripotent stem cells, embryonal carcinoma stem cells, hemangioblasts, lymphoid progenitor cells, *etc.*

INDEXING/ABSTRACTING

The *WJSC* is now abstracted and indexed in Science Citation Index Expanded (SCIE, also known as SciSearch®), Journal Citation Reports/Science Edition, PubMed, PubMed Central, Scopus, Biological Abstracts, BIOSIS Previews, Reference Citation Analysis, China Science and Technology Journal Database, and Superstar Journals Database. The 2023 Edition of Journal Citation Reports® cites the 2022 impact factor (IF) for *WJSC* as 4.1; IF without journal self cites: 3.9; 5-year IF: 4.5; Journal Citation Indicator: 0.53; Ranking: 15 among 29 journals in cell and tissue engineering; Quartile category: Q3; Ranking: 99 among 191 journals in cell biology; and Quartile category: Q3. The *WJSC*'s CiteScore for 2022 is 8.0 and Scopus CiteScore rank 2022: Histology is 9/57; Genetics is 68/325; Genetics (clinical) is 19/90; Molecular Biology is 119/380; Cell Biology is 95/274.

RESPONSIBLE EDITORS FOR THIS ISSUE

Production Editor: *Xiang-Di Zhang*; Production Department Director: *Xu Guo*; Editorial Office Director: *Jia-Ru Fan*.

NAME OF JOURNAL

World Journal of Stem Cells

ISSN

ISSN 1948-0210 (online)

LAUNCH DATE

December 31, 2009

FREQUENCY

Monthly

EDITORS-IN-CHIEF

Shengwen Calvin Li, Carlo Ventura

EDITORIAL BOARD MEMBERS

<https://www.wjgnet.com/1948-0210/editorialboard.htm>

PUBLICATION DATE

February 26, 2024

COPYRIGHT

© 2024 Baishideng Publishing Group Inc

INSTRUCTIONS TO AUTHORS

<https://www.wjgnet.com/bpg/gerinfo/204>

GUIDELINES FOR ETHICS DOCUMENTS

<https://www.wjgnet.com/bpg/GerInfo/287>

GUIDELINES FOR NON-NATIVE SPEAKERS OF ENGLISH

<https://www.wjgnet.com/bpg/gerinfo/240>

PUBLICATION ETHICS

<https://www.wjgnet.com/bpg/GerInfo/288>

PUBLICATION MISCONDUCT

<https://www.wjgnet.com/bpg/gerinfo/208>

ARTICLE PROCESSING CHARGE

<https://www.wjgnet.com/bpg/gerinfo/242>

STEPS FOR SUBMITTING MANUSCRIPTS

<https://www.wjgnet.com/bpg/GerInfo/239>

ONLINE SUBMISSION

<https://www.f6publishing.com>

Basic Study

VX-509 attenuates the stemness characteristics of colorectal cancer stem-like cells by regulating the epithelial-mesenchymal transition through Nodal/Smad2/3 signaling

Yun Yuan, Xu-Fan Zhang, Yu-Chen Li, Hong-Qing Chen, Tian Wen, Jia-Lian Zheng, Zi-Yi Zhao, Qiong-Ying Hu

Specialty type: Cell and tissue engineering

Provenance and peer review:

Unsolicited article; Externally peer reviewed.

Peer-review model: Single blind

Peer-review report's scientific quality classification

Grade A (Excellent): 0

Grade B (Very good): 0

Grade C (Good): C, C

Grade D (Fair): 0

Grade E (Poor): 0

P-Reviewer: Ventura C, Italy

Received: October 30, 2023

Peer-review started: October 30, 2023

First decision: December 5, 2023

Revised: December 19, 2023

Accepted: January 16, 2024

Article in press: January 16, 2024

Published online: February 26, 2024



Yun Yuan, Yu-Chen Li, Hong-Qing Chen, Tian Wen, Qiong-Ying Hu, Department of Laboratory Medicine, Hospital of Chengdu University of Traditional Chinese Medicine, Chengdu 610072, Sichuan Province, China

Xu-Fan Zhang, Department of Nuclear Medicine, Hospital of Chengdu University of Traditional Chinese Medicine, Chengdu 610072, Sichuan Province, China

Xu-Fan Zhang, College of Medical Technology, Chengdu University of Traditional Chinese Medicine, Chengdu 611137, Sichuan Province, China

Jia-Lian Zheng, Department of Hepatology, Affiliated Hospital of Liaoning University of Traditional Chinese Medicine, Shenyang 110032, Liaoning Province, China

Zi-Yi Zhao, Hospital of Chengdu University of Traditional Chinese Medicine, Chengdu 610072, Sichuan Province, China

Zi-Yi Zhao, Traditional Chinese Medicine Regulating Metabolic Diseases Key Laboratory of Sichuan Province, Chengdu 610072, Sichuan Province, China

Corresponding author: Qiong-Ying Hu, PhD, Associate Professor, Department of Laboratory Medicine, Hospital of Chengdu University of Traditional Chinese Medicine, No. 39 Shierqiao Road, Jinniu District, Chengdu 610072, Sichuan Province, China. qiongyinghu@163.com

Abstract**BACKGROUND**

Colorectal cancer stem cells (CCSCs) are heterogeneous cells that can self-renew and undergo multidirectional differentiation in colorectal cancer (CRC) patients. CCSCs are generally accepted to be important sources of CRC and are responsible for the progression, metastasis, and therapeutic resistance of CRC. Therefore, targeting this specific subpopulation has been recognized as a promising strategy for overcoming CRC.

AIM

To investigate the effect of VX-509 on CCSCs and elucidate the underlying mechanism.

METHODS

CCSCs were enriched from CRC cell lines by in conditioned serum-free medium. Western blot, Aldefluor, transwell and tumorigenesis assays were performed to verify the phenotypic characteristics of the CCSCs. The anticancer efficacy of VX-509 was assessed in HCT116 CCSCs and HT29 CCSCs by performing cell viability analysis, colony formation, sphere formation, flow cytometry, and western blotting assessments *in vitro* and tumor growth, immunohistochemistry and immunofluorescence assessments *in vivo*.

RESULTS

Compared with parental cells, sphere cells derived from HCT116 and HT29 cells presented increased expression of stem cell transcription factors and stem cell markers and were more potent at promoting migration and tumorigenesis, demonstrating that the CRC sphere cells displayed CSC features. VX-509 inhibited the tumor malignant biological behavior of CRC-stem-like cells, as indicated by their proliferation, migration and clonality *in vitro*, and suppressed the tumor of CCSC-derived xenograft tumors *in vivo*. Besides, VX-509 suppressed the CSC characteristics of CRC-stem-like cells and inhibited the progression of epithelial-mesenchymal transition (EMT) signaling *in vitro*. Nodal was identified as the regulatory factor of VX-509 on CRC stem-like cells through analyses of differentially expressed genes and CSC-related database information. VX-509 markedly downregulated the expression of Nodal and its downstream phosphorylated Smad2/3 to inhibit EMT progression. Moreover, VX-509 reversed the dedifferentiation of CCSCs and inhibited the progression of EMT induced by Nodal overexpression.

CONCLUSION

VX-509 prevents the EMT process in CCSCs by inhibiting the transcription and protein expression of Nodal, and inhibits the dedifferentiated self-renewal of CCSCs.

Key Words: Colorectal cancer stem cells; Stemness; VX-509; Epithelial-mesenchymal transition; Nodal

©The Author(s) 2024. Published by Baishideng Publishing Group Inc. All rights reserved.

Core Tip: Colorectal cancer (CRC) is a malignant cancer of the digestive tract with high recurrence and metastasis. CRC stem cells (CCSCs) exerted self-renewing and repopulating capacity, which are hard to eliminate and cause recurrence and metastasis of CRC. VX-509 has been reported as a rheumatoid arthritis regular treatment. However, the role of VX-509 in CCSCs is not well studied. In this study, VX-509 inhibited the malignant biological behaviors and stemness of CCSCs. Further experiments suggested that VX-509 downregulated the expression of Nodal to suppress the epithelial-mesenchymal transition and inhibit the stemness of CCSCs, which provided a potent therapy measure for CRC.

Citation: Yuan Y, Zhang XF, Li YC, Chen HQ, Wen T, Zheng JL, Zhao ZY, Hu QY. VX-509 attenuates the stemness characteristics of colorectal cancer stem-like cells by regulating the epithelial-mesenchymal transition through Nodal/Smad2/3 signaling. *World J Stem Cells* 2024; 16(2): 207-227

URL: <https://www.wjgnet.com/1948-0210/full/v16/i2/207.htm>

DOI: <https://dx.doi.org/10.4252/wjsc.v16.i2.207>

INTRODUCTION

Colorectal cancer (CRC) is a globally prevalent malignant disease with a significant increase in incidence. By 2020, about 1.93 million individuals had been diagnosed with new cases of CRC, and an estimated 900000 deaths were reported among all CRC patients[1]. Considering the global demographic projections based on the human development index, 3.2 million new CRC cases and 1.6 million deaths are predicted to occur worldwide by 2040[2]. Despite the availability of relatively advanced diagnostic screening methods and treatments, CRC patients continue to face poor outcomes characterized by ineffective early-stage diagnosis, recurrence and metastasis due to incomplete tumor removal, and resistance to chemoradiotherapy[3].

Cancer stem cells (CSCs) are a rare and heterogeneous population of cells within tumors, that possess self-renewal ability and the capacity for multidirectional differentiation[4]. CSCs can be differentiated into malignant tumor cells upon stimulation of the tumor microenvironment[5]. The essence of CSCs is cell plasticity, which endows CSCs with the potential for aberrant cell proliferation and differentiation to adapt to various internal environments and break through the human immune barrier, eventually leading to relapse, metastasis, and multidrug resistance in CRC[6]. Colorectal cancer stem cells (CCSCs) were initially identified in the immunodeficient mice that underwent renal capsule transplantation[7]. CCSCs, which are distinct from CRC cells, strongly support disordered tumor growth and treatment resistance and are considered to be an important source of drug-resistant cells that contribute to tumor recurrence and metastasis following chemotherapy-induced remission[8]. Conventional treatment targets the malignant proliferation of CRC cells, while targeting CCSCs can be an effective strategy for eradicating CRC from the source.

Several studies have reported that epithelial-mesenchymal transition (EMT) induces cancer cells to obtain stemness from CSCs during the progression of malignancy[9-11]. Zhu *et al*[12] reported that Snai1 overexpression sustained stemness maintenance and confers a radiation-resistant phenotype in CRC cells. Transforming growth factor- β (TGF- β) signaling is the most classical pathway that is known to induce EMT and acts a dominant role through various intracellular factors. Nodal, a member of the TGF- β superfamily, has been identified as an embryonic morphogen[13]. Overexpression of Nodal in malignant cancer cells enhances the invasiveness and migration of tumors, accompanied by phenotypic protein alterations[14]. A recent study demonstrated that Nodal is specifically expressed in CD44⁺/CD24⁺ CRC cells and promotes the formation of CCSC spheroids by activating Smad2/3 phosphorylation to promote the self-renewal of CCSCs[15]. Therefore, the regulation of EMT signaling may serve as a key mechanism underlying the maintenance of CSC stemness.

VX-509 (decernotinib), a selective inhibitor of Janus kinase 3 (JAK3), modulates lymphocyte survival and proliferation by blocking the cytokine activities of interleukin (IL)-2, IL-4, IL-7 and IL-15[16-18]. A phase II clinical trial of VX-509 for the treatment of rheumatoid arthritis (RA) demonstrated that combining VX-509 with disease-modifying antirheumatic drugs effectively improved RA[19]. Several studies have shown that other JAK3 inhibitors are effective in treating CRC *in vivo* in animal models and in inducing apoptosis and putative CSC cycle arrest in CRC *in vitro*[20-23]. VX-509 is currently considered as a traditional RA treatment and topical formulation for psoriasis, but its effect on cancer remains unknown. Here, we designed our study to screen various inhibitors for their effects on a CRC stem-like cell model and relevant animal models. This study allowed us to identify the potent anticancer efficacy of VX-509 by inhibiting the stemness of CSCs, endowing VX-509 with greater therapeutic value. We characterized the phenotypic traits of CRC-derived CSCs, evaluated the therapeutic efficacy of VX-509 through various experiments, and investigated the underlying signaling pathways involved in these processes.

MATERIALS AND METHODS

Reagents

For *in vitro* studies, VX-509 (Cat# B5929, APE \times BIO, United States) was dissolved in dimethyl sulfoxide (DMSO, MP Biomedicals, United States) at a stock solution concentration of 10 mmol/L. For *in vivo* studies, VX-509 was dissolved in the mixture containing DMSO and 5% sodium carboxymethylcellulose (CMC). Recombinant Nodal recombinant homolog was purchased from Zeye company (Shanghai, China). Nodal recombinant protein was prepared as stock solutions in phosphate-buffered saline (PBS) prior to diluting in cell culture medium. For antibodies, Oct-4 (Cat# 381335, ZEN-BIOSCIENCE, Chengdu, China), Nanog (Cat# 381167) and SOX2 (Cat# 864316) were purchased from ZEN-BIOSCIENCE; CD133 (Cat# ab216323), CD44 (Cat# ab189524) and Nodal (Cat# ab55676) were purchased from Abcam; β -actin (Cat# 20536-1-AP) and GAPDH (Cat# 10494-1-AP) were purchased from Proteintech; E-cadherin (Cat# AF6759), N-cadherin (Cat# AF5237), vimentin (Cat# AF1975), JAK3 (Cat# AF7314), p-Smad2/3 (Cat# AF5920), goat anti-rabbit immunoglobulin (Ig)G antibody (Cat# A0208) and goat anti-mouse IgG antibody (Cat# A0216) were purchased from Beyotime.

Cell culture

The human CRC cell lines HCT116 and HT29 were acquired from the American Type Culture Collection. Cells were maintained in high-glucose Dulbecco's modified Eagle's medium (DMEM, Gibco, NY, United States) containing 10% fetal bovine serum (FBS, Gibco, NY, United States) and incubated at 37 °C with 95% humidity and 5% CO₂.

Enrichment of cancer stem-like cells

Cells were cultured in serum free medium (SFM) as previously reported to enrich CSCs from HCT116 and HT29[24]. The SFM consisted of DMEM/F12 medium (Life Technologies, United States) supplemented with 20 ng/mL epidermal growth factor (EGF, Invitrogen, United States), 10 ng/mL basic fibroblast growth factor (bFGF, Invitrogen, United States), 2% B27 supplement (Life Technologies, USA) in 6-well ultra-low-adherent plates (Cat#3471, Corning, NY, United States). Culture medium was replaced twice a week, and CSCs were passaged every six to seven days using TrypLE (Gibco, NY, United States).

Western blot analysis

After lysis, the cell protein concentrations were measured using BCA Protein Assay Kit (Cat# P0012S, Beyotime, Shanghai, China). 20 μ g proteins were separated on 10% sodium-dodecyl sulfate gel electrophoresis and transferred onto polyvinylidene fluoride membranes (Thermo Fisher Scientific, United States). The membranes were blocked with 5% non-fat milk in Tris-HCl buffer saline supplemented with 0.1% Tween-20 (TBS-T) at room temperature for 30-45 min, and then incubated with primary antibodies (dilution 1:1000) at 4 °C overnight. Subsequently, the membranes were washed with TBS-T for three times and incubated with secondary antibodies (dilution 1:5000) at 37 °C for 2 h. After washing for three times, immunoreactive bands were caught using electrochemiluminescence reagent (Cat# 4AW011, 4A Biotech, Beijing, China) and quantified using ImageJ software.

Aldefluor assay

ALDEFUOR™ is a non-immunological fluorescent reagent system that has been used to detect high expression of aldehyde dehydrogenase (ALDH)-bright cells from normal and cancer stem and progenitor cells of various lineages. It has been reported that CRC cells with high ALDH expression showed stronger cancer stemness, and ALDH activity has

been widely used as a marker of CCSCs[25-28]. After washed with PBS twice, 10^6 cells were suspended in 1 mL assay buffer. 1 mL sample suspension was placed into the test tube. And 5 μ L ALDEFLUOR™ DEAB reagent was added into the control tube, while 5 μ L activated ALDEFLUOR™ reagent was added into the test tube. Then, 0.5 mL mixed solution was transferred from the test tube to the control tube. After incubation for 30 min at 37 °C, all tubes were centrifuged at 250 g for 5 min, and the supernatant was removed. After adding 0.5 mL ALDEFLUOR™ Assay Buffer, all the samples were detected by using Navios flow cytometer (Beckman Coulter, Brea, United States). The data were analysed using FlowJo 10.4 software (FlowJo LLC, Ashland, United States).

Cell viability analysis

Cells (2×10^4 cells/100 μ L) seeded in 96-well plates were treated with various concentrations of VX-509 for 24h. Then, 10 μ L cell counting kit-8 (CCK-8) (AbMole, Shanghai, China) solution was added to each well for 2 h at 37 °C. The optical density (OD) at 450 nm was analyzed using a multifunctional microplate reader (FlexStation 3, Molecular Devices).

Annexin V/PI double staining apoptosis analysis

All cells (5×10^5 cells/2 mL) seeded in 6-well ultra-low-adherent plates were treated with various concentrations of VX-509 for 24 h. Apoptosis was measured using Annexin V/PI analysis kit (Cat# A211-02, Vazyme, Nanjing, China). Briefly, cells were dissociated and resuspended in 0.1 mL $1 \times$ binding buffer. Next, 5 μ L FITC Annexin V-FITC and 5 μ L PI staining solution were added, followed by incubation at room temperature for 10 min. After adding 0.4 mL $1 \times$ binding buffer, all the samples were detected by using Navios flow cytometer (Beckman Coulter, Brea, United States). The data were analysed using FlowJo 10.4 software (FlowJo LLC, Ashland, United States).

Cell cycle analysis

Cells (5×10^5 cells/2 mL/well) seeded in 6-well ultra-low-adherent plates were treated with various concentrations of VX-509 for 24 h. Cell cycle analysis was measured by cell cycle and apoptosis analysis kit (Cat# C1052, Beyotime, Shanghai, China). After fixation with 70% ethanol, cells were incubated with 0.5 mL propidium iodide staining solution at 37 °C for 30 min. The cell cycle was detected by using Navios flow cytometer (Beckman Coulter, Brea, United States). The data were analysed using FlowJo 10.4 (FlowJo LLC, Ashland, United States).

Transwell migration analysis

Cell migration was examined using the 24-well transwell culture plates (Cat#3422, Corning, NY, United States). Cells (10^5 cells/100 μ L/well) were plated in the top chamber with SFM (without serum or growth factors) containing various concentrations of VX-509 or DMSO. And the medium supplemented with DMEM and 10% FBS was used as a chemoattractant in the lower chamber. After 48 h, cells on the lower surface of the membrane were fixed with paraformaldehyde and stained with crystal violet. Finally, 5 images (100 \times) were randomly collected by image acquisition microscopy (IX71, Olympus, Tokyo, Japan).

Soft agar clonal assay

0.6% agarose in SFM was overlaid on the bottom of 6-well plates. Dissociated cells (5×10^3 /well) were suspended in SFM containing 0.3% agarose and placed on the top of the bottom layer. Cells were treated with different concentrations of VX-509 for 3 wk. 50 μ L SFM without any treatment were added every 3 d. After 3 wk, 200 μ L Nitroterazolium Blue chloride (Solarbio, Beijing, China) was added to each well. After 4 h, the number of colonies was counted under the microscopy.

Sphere formation and recovery assay

For formation assay, cells (2×10^4 /well) were seeded in 2 mL SFM in 6-well ultra-low-adherent plates and treated with different concentrations of VX-509 or DMSO. After incubating at 37 °C for 5 d, pictures were taken under the microscopy and tumor spheres were counted in five fields.

For recovery assay, cells were treated with different concentrations of VX-509 or DMSO. After 72 h, cells from each group were collected and digested into single cell. Subsequently, for each group, cells (2×10^4 /well) were seeded in 6-well ultra-low-adherent plates in SFM medium condition without VX-509 or DMSO. After incubating at 37 °C for 5 d, pictures were taken under the microscopy and tumor spheres were counted in five fields.

Animal experiments

All the animal experiments were approved by the ethics committee of the Institutional Animal Care and Use Committee of Institute of Chengdu University of Traditional Chinese Medicine. 4-6-wk-old female BALA/-c nude mice were purchased from Vital River Laboratory Animal Technology Company (Beijing, China) and fed in the specific pathogen free room of the Experimental Animal Center of Chengdu Medical College. For *in vivo* tumorigenesis analysis, 5×10^5 HCT116 CSCs and 5×10^5 HCT116 cells were dissociated into single cell suspensions diluted in DMEM/F12. Then, they were subcutaneously implanted in the right and left flanks of nude mice. There were 5 nude mice in each group. Tumor growth was observed and recorded twice a week. The mice were sacrificed after 3 months. For *in vivo* analysis, 5×10^5 HCT116 CSCs were subcutaneously implanted in the right flanks of nude mice. The tumor-bearing mice were randomly divided into three groups (5 mice/group) when the average tumor volume reached 60-70 mm³. The mice in each group were orally administered with 50 mg/kg, 100 mg/kg VX-509 (dissolved in DMSO and 0.5% CMC) or vehicle every other day. Tumor volume (V) was measured every other day using caliper and calculated using the following formula: V (mm³) = $(L \times W^2)/2$, where L = length (mm), W = width (mm). The animals were sacrificed 14 d later and the tumor tissues were obtained for subsequent experiments.

Immunohistochemistry

After deparaffinization and rehydration, the sections were incubated with sodium citrate buffer at 100 °C for 15 min. Subsequently, the sections were treated with 3% H₂O₂ and blocked with 10% goat serum at room temperature for 1 h. Following this, the sections were incubated overnight at 4 °C with Ki67, TUNEL or vimentin antibodies. Horseradish peroxidase-labelled secondary antibody was then applied to the slices. The signals were visualized using the 3,3'-diaminobenzidine (DAB) reagent, where blue color represented hematoxylin and brown color represented DAB staining. All images were acquired using microscopy. The mean of the integrated IOD was analyzed using the ImageJ software.

Immunofluorescence

The tumor tissues were fixed in ice-cold 4% paraformaldehyde overnight at 4 °C and subsequently equilibrated in 30% sucrose solution. Sections were then washed for three times with cold PBS, blocked with 5% goat serum for 1 h, and incubated overnight at 4 °C with a primary antibody against SOX2 (diluted to 1:500). After incubating with secondary antibody for 1 h at room temperature, all the slices were counterstained with DAPI, and photomicrographs were captured using an Olympus DP70 digital camera and software (Olympus, Japan) or a confocal microscopy (Nikon, Japan). The mean of the integrated IOD was analyzed using the ImageJ software.

RNA sequencing, transcriptome data analysis and annotation

HT29 CSCs from two groups (control and VX-509 treated) were subjected to total RNA extraction using TRIzol reagent (Thermo Fisher Scientific, United States), according to the manufacturer's instructions. 1 µg of high-quality RNA/group was used to generate libraries and was sequenced using a NovaSeq 6000 sequencer (Illumina Inc., San Diego, United States) at Biozeron Co., Ltd. (Shanghai, China). The Illumina paired-end sequencing service was provided by Shanghai Ling En Biotechnology Co., Ltd., Shanghai, China. Multiple testing hypothesis correction was performed to estimate relative expression levels. An adjusted *P*-value < 0.05 and |log₂ fold change| ≥ 1 were used as the threshold parameters of significantly differentially expressed genes (DEGs). Functional annotation was performed according to the Gene Ontology (GO) terms and the Kyoto Encyclopedia of Genes and Genomes. Pathway analysis was performed in the Molecular Signature Database v7.0 (MSigDB), to systematically explore the functions of DEGs.

Real-time quantitative polymerase chain reaction

Total RNA was extracted by using the TRIzol reagent. After isolation, the concentration of purified RNA was determined by the UV spectrophotometer (Life Technologies, Grand Island, NY, United States). cDNA was reverse-transcribed from the extracted total RNA using the SureScript™ First-Strand cDNA Synthesis kit (GeneCopoeia, Guangzhou, China). BlazeTaq™ SYBR Green qPCR Mix 2.0 (GeneCopoeia, Guangzhou, China) was used in ABI 7500 system (Applied Biosystems, Foster City, CA, United States) under the following conditions: 95 °C 10 min, 60 cycles of 95 °C 15 s, and 60 °C 1 min. The specific primers used were as follows: GAPDH forward: 5'-GCTCAGACACCATGGGGAAG-3'; reverse: 5'-TGTAGTTGAGGTCAATGAAGGGG-3'; Nodal forward: 5'-GGCGAGTGTCTAATCCTGTTG-3'; reverse: 5'-CGTTTCAGCAGACTCTG-3'.

Statistics

The data were presented as mean ± standard error of mean. Student's *t*-test or one-way ANOVA followed by Bonferroni test was employed to compare two independent variables using GraphPad Prism (Version 8.0.1).

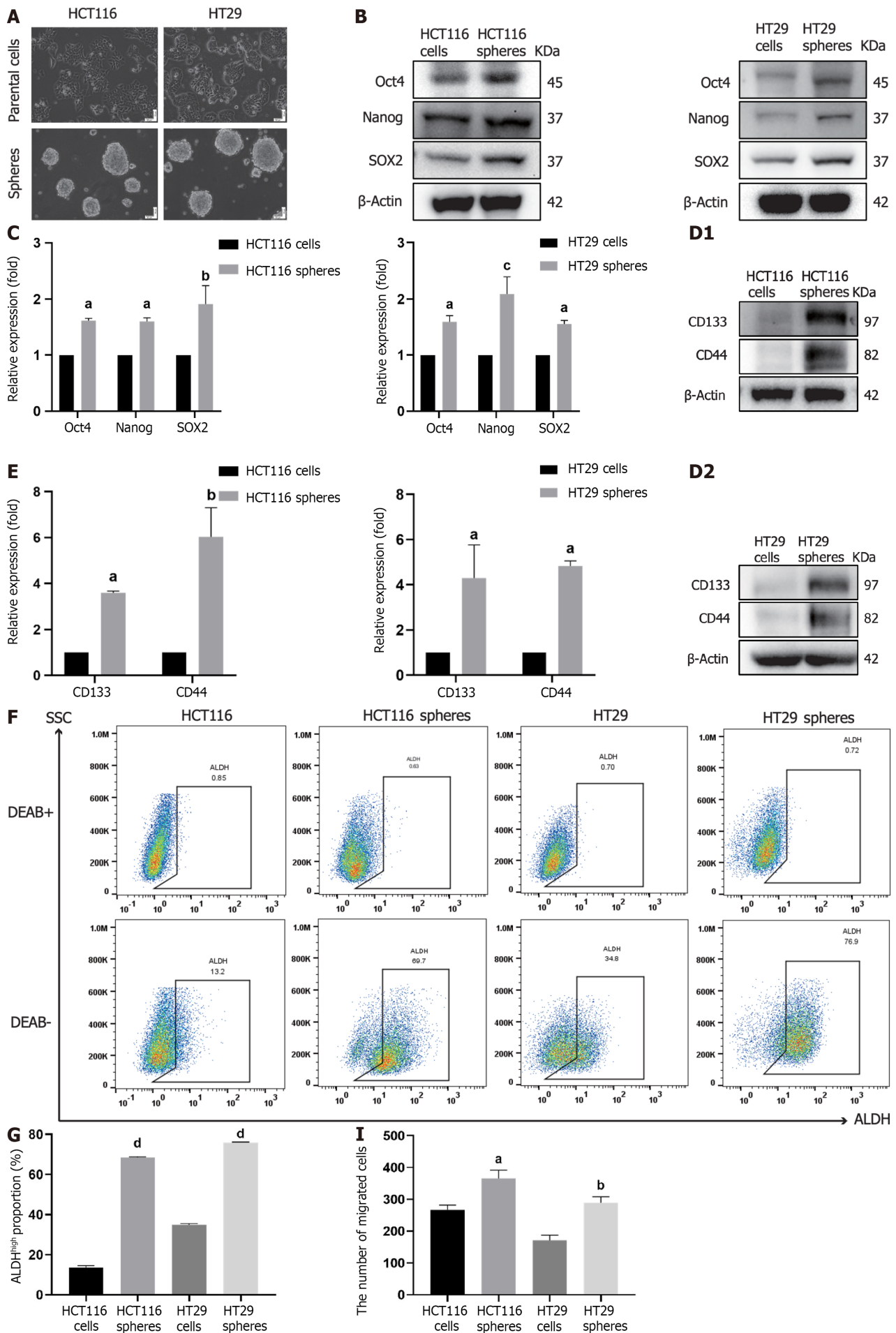
RESULTS

Establishment and identification of HCT116 and HT29 cell line-derived CCSCs

CCSCs are malignant cell subpopulations of CRC solid tumors; one of the effective acquisition methods for these cells is SFM suspension culture[29]. Based on the experimental requirements, we cultured the human colorectal cell lines HCT116 and HT29 in SFM culture conditions to enrich related CCSCs. After five passages in culture, numerous spheroid clusters were observed *via* microscopy (Figure 1A). To explore the difference in cancer stemness between parental cells and sphere cells, we collected these cells and detected the expression of stem cell transcription factors and stem cell markers. The sphere cells exhibited higher expression of Oct4, Nanog, SOX2, CD133 and CD44 than did the parental cells (Figure 1B-E). Furthermore, flow cytometry results for ALDH detection showed that, compared with their parental cells, more sphere cells were positive for ALDH (Figure 1F and G). Enhanced tumor invasion is a typical malignant characteristic of CSCs, as shown in Figure 1H and I. Increased cells were observed in the transwell plates for the sphere groups. To explore the difference in tumor formation between parental cells and sphere cells *in vivo*, HCT116 parental cells and HCT116 sphere cells were subcutaneously implanted into the flanks of immunodeficient mice. As expected, more obvious tumor nodules developed on the sphere cell implantation side than on the parental cell implantation side (Figure 1J). Taken together, these results suggested that the sphere cells derived from HCT116 and HT29 cells were enriched successfully and possessed CCSC characteristics for use in subsequent experiments.

VX-509 inhibited the tumor malignant biological behavior of CRC stem-like cells

Based on the previous screening experiment, we explored the effect of VX-509 on CRC stem-like cells. Primarily, cell viability was assessed, and VX-509 inhibited the proliferation of HCT116 CSCs and HT29 CSCs in a dose-dependent manner (Figure 2A). The results showed that the half-maximal inhibitory concentration (IC₅₀) of VX-509 on HCT116 CSCs



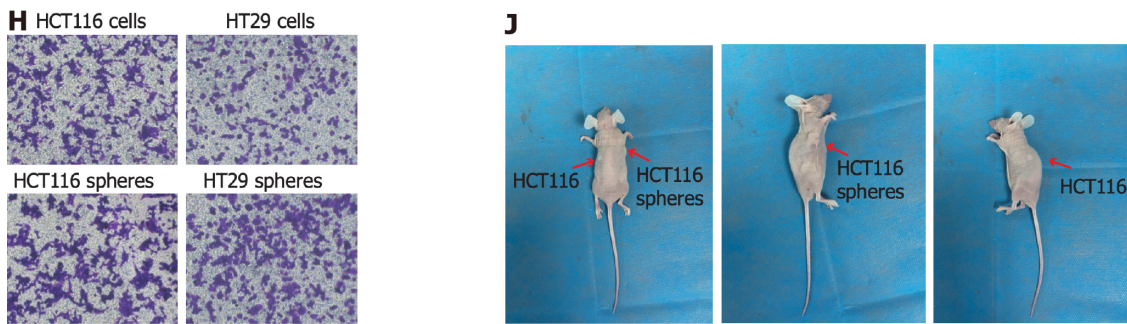


Figure 1 Spherical cells derived from colorectal cancer cell lines exhibit cancer stem cell characteristics. A: Microscopy images of colorectal cancer parental cells and specified serum free cultured spheres; B-E: The protein expression levels of Oct4, Nanog, and SOX2 (B), CD133 and CD44 (D) in parental cells and sphere cells are shown. Densitometric analysis of Oct4, Nanog, and SOX2 (C) and CD133 and CD44 (E) normalized against β -Actin; F and G: ALDH⁺ cells were measured using flow cytometry and relative statistical analysis; H and I: Transwell migration assay of parental cells and sphere cells and relative statistical analysis; J: Representative pictures showing the tumorigenic capacities of parental cells and sphere cells derived from HCT116 cells. Scale bar = 50 μ m. $n = 3$. ^a $P < 0.05$, ^b $P < 0.01$, ^c $P < 0.001$, ^d $P < 0.0001$ compared to the HCT116 cell group and HT29 cell group. ALDH: Aldehyde dehydrogenase.

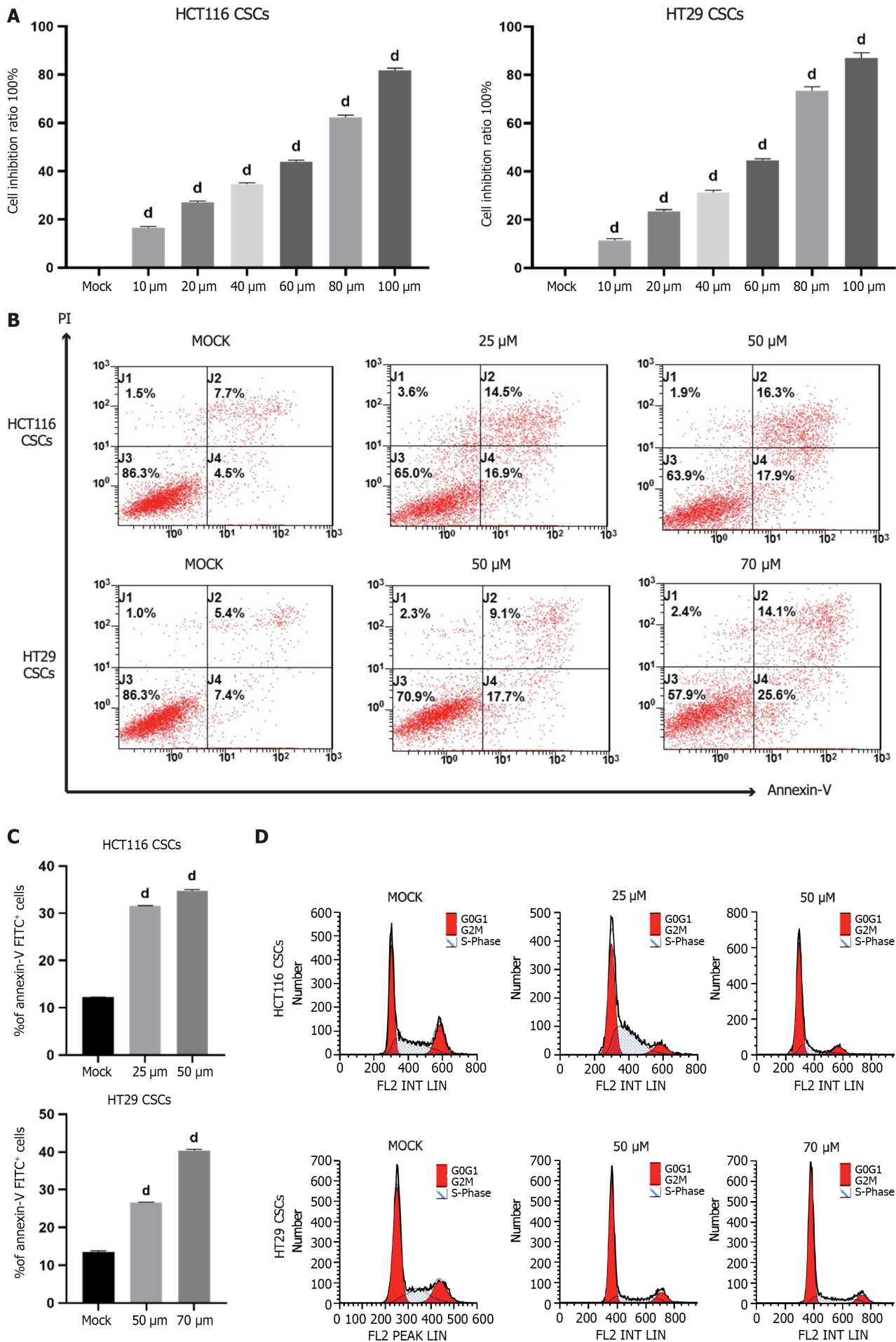
was 50 μ M, and the 30% inhibitory concentration (IC_{30}) was 25 μ M. For HT29 CSCs, the IC_{50} was 70 μ M, and the IC_{30} was 50 μ M. Furthermore, the results of Annexin V-FITC/PI staining and flow cytometry showed that the number of apoptotic cells increased and the number of G2/M phase cells decreased significantly after VX-509 treatment, indicating that VX-509 can induce DNA damage and G2/M phase cell cycle arrest, eventually inducing apoptosis (Figure 2B-E). Besides, the results of transwell experiments showed that VX-509 inhibited the migration of HCT116 CSCs and HT29 CSCs (Figure 2F and G). The number of cell colonies decreased after VX-509 treatment, indicating that VX-509 had negative effects on the population dependence and proliferation ability of HCT116 CSCs and HT29 CSCs (Figure 2H and I). In conclusion, these results revealed that VX-509 exhibits a potent anticancer effect on the CRC stem-like cells.

VX-509 suppressed the stemness of CRC stem-like cells and differentiated CRC stem-like cells into CRC cells by inhibiting EMT signaling

In the previous screening experiment, CRC stem-like cells were treated with different concentrations of VX-509. At 30 μ M, HCT116 CSCs markedly differentiated into epithelioid CRC cells, while at 50 μ M, HT29 CSCs markedly differentiated into epithelioid CRC cells. This study further examined the effects of these concentrations of VX-509 on the stemness of HCT116 CSCs and HT29 CSCs. As shown in Figure 3A and B, treatment of CRC stem-like cells with VX-509 for 5 d resulted in significant decreases in the number and size of the spheres. To verify whether the inhibition was reversible, HCT116 CSCs and HT29 CSCs were pretreated with different concentrations of VX-509 for 3 d before they were dissociated into single cells and cultured in SFM for 5 d. Consistently, VX-509 treatment decreased both the number and size of the spheres (Figure 3C and D). In addition, the protein expression of key stem cell transcription factors (Oct4, Nanog, and SOX2) in HCT116 CSCs and HT29 CSCs reduced markedly after VX-509 administration (Figure 3E and F). Obvious morphologic changes in CRC stem-like cells were observed after VX-509 treatment, and CCSCs dedifferentiation was detected in regular 6-well plates (Figure 3G). Since EMT transformation drives cancer cells to dedifferentiate into CSCs by improving cell plasticity[30], we decided to investigate whether the inhibitory effect elicited by VX-509 on CSCs may involve changes in EMT patterning. A well-known hallmark of EMT is the upregulation of N-cadherin followed by the downregulation of E-cadherin. Consistent with our hypothesis, compared with mock treatment, VX-509 treatment remarkably changed the expression patterns of EMT related proteins by eliciting the upregulation of E-cadherin while inhibiting the expression of N-cadherin and vimentin (Figure 3H and I). To summarize, VX-509 inhibited the stemness of CRC stem-like cells in relation to the attenuation of EMT progression.

VX-509 exerted anticancer effects on CRC stem-like cell xenografts in vivo

Based on the observation that treatment with VX-509 could diminish the malignant behaviors and stemness of CRC stem-like cells *in vitro*, further tests of VX-509 on CRC stem-like cells *in vivo* were carried out. CRC stem-like cells were subcutaneously implanted into the right flanks of immunodeficient mice (5×10^5 cells per mouse). The mice were randomly divided into a control group and 50 and 100 mg/kg VX-509 groups (5 mice/group). As shown in Figure 4A-C, compared with those in the control group, the mean tumor volumes and mean tumor weights in the 50 and 100 mg/kg VX-509 groups markedly decreased. Moreover, Ki67 staining revealed that significant decreases in Ki67-positive cells in the 50 and 100 mg/kg VX-509 groups (Figure 4D and E). TUNEL staining revealed increased numbers of TUNEL-positive cells in CRC stem like-cells xenografts in the 50 and 100 mg/kg VX-509 groups (Figure 4F and G). These data indicated that VX-509 treatment could suppress tumor growth and induce cell apoptosis. Next, we investigated whether VX-509 treatment affects the expression of stem cell transcription-related proteins. As shown in Figure 4H and I, the immunofluorescence staining assay data suggested that VX-509 treatment distinctly inhibited SOX2-positive cells in CRC stem-like cell-implanted tumors. In addition, the expression of vimentin, an EMT related protein, was also suppressed by VX-509 treatment as compared with that in the control group (Figure 4J and K). Taken together, these results illustrated that the obvious anticancer effect of VX-509 on CRC stem-like cells *in vivo*.



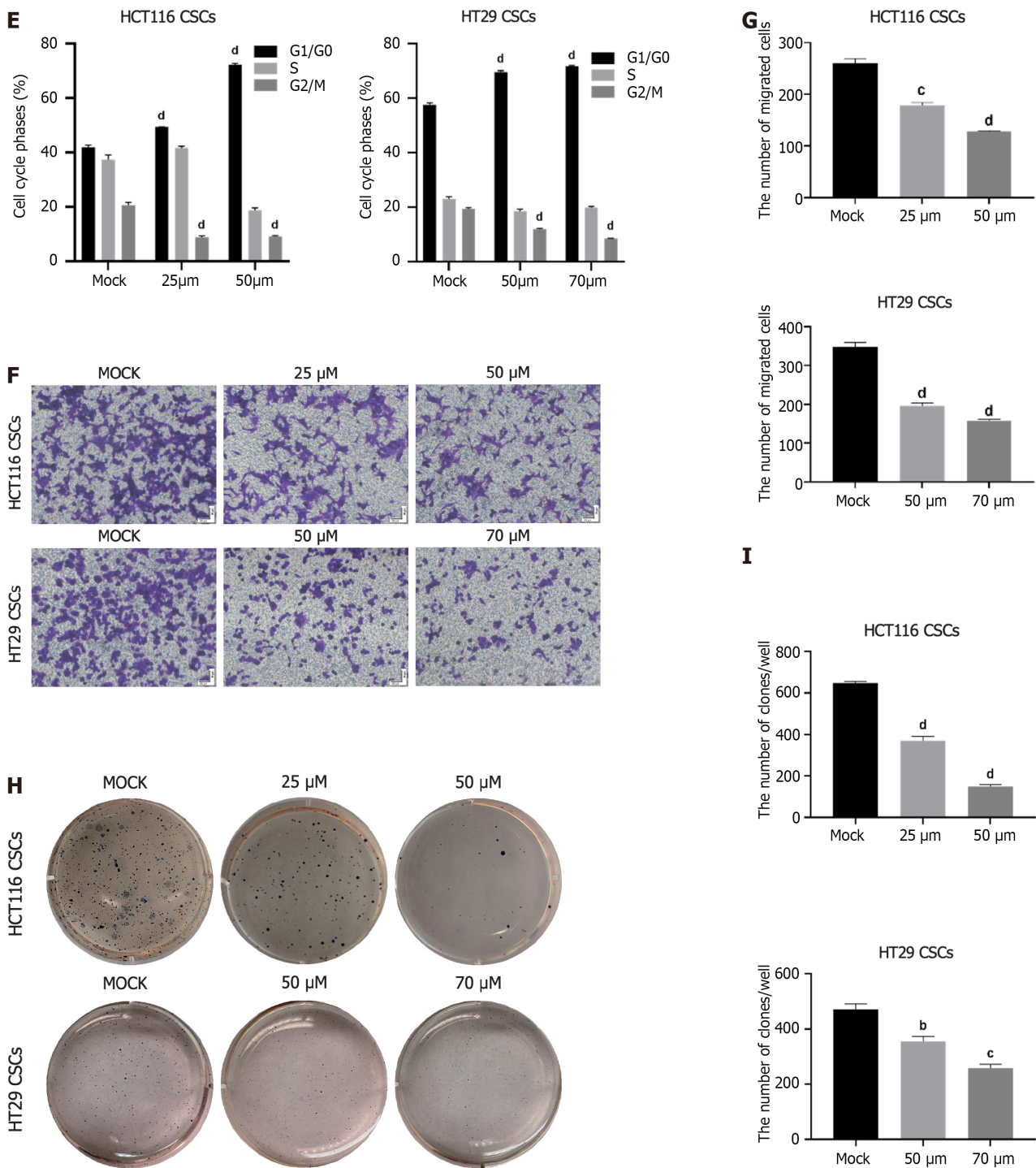


Figure 2 VX-509 inhibits the growth, migration, invasion and clonogenicity of colorectal cancer-derived cancer stem cells. A: The viability of colorectal cancer-derived cancer stem cells (CSCs) treated with different concentrations of VX-509 was measured by a cell counting kit-8 assay; B and C: Flow cytometry analysis of early and late apoptotic rates and relative statistical analysis; D: Cell cycle distribution was measured using flow cytometry; E: Histograms of the proportions of G0/G1-, S- and G2/M-phase cells; F and G: The effects of different concentrations of VX-509 on the migration of HCT116 CSCs and HT29 CSCs detected by transwell assays and relative statistical analysis; H and I: The effects of different concentrations of VX-509 on the proliferation and tumorigenesis of HCT116 CSCs and HT29 CSCs detected by soft agar colony formation assays and relative statistical analysis. Scale bar = 50 μm. *n* = 3. ^b*P* < 0.01, ^c*P* < 0.001, ^d*P* < 0.0001 compared to the HCT116 cancer stem cells Mock group and HT29 cancer stem cells Mock group. CSC: Cancer stem cell.

VX-509 inhibited the phosphorylation of Smad2/3 to suppress EMT progression by downregulating Nodal in CRC stem-like cells

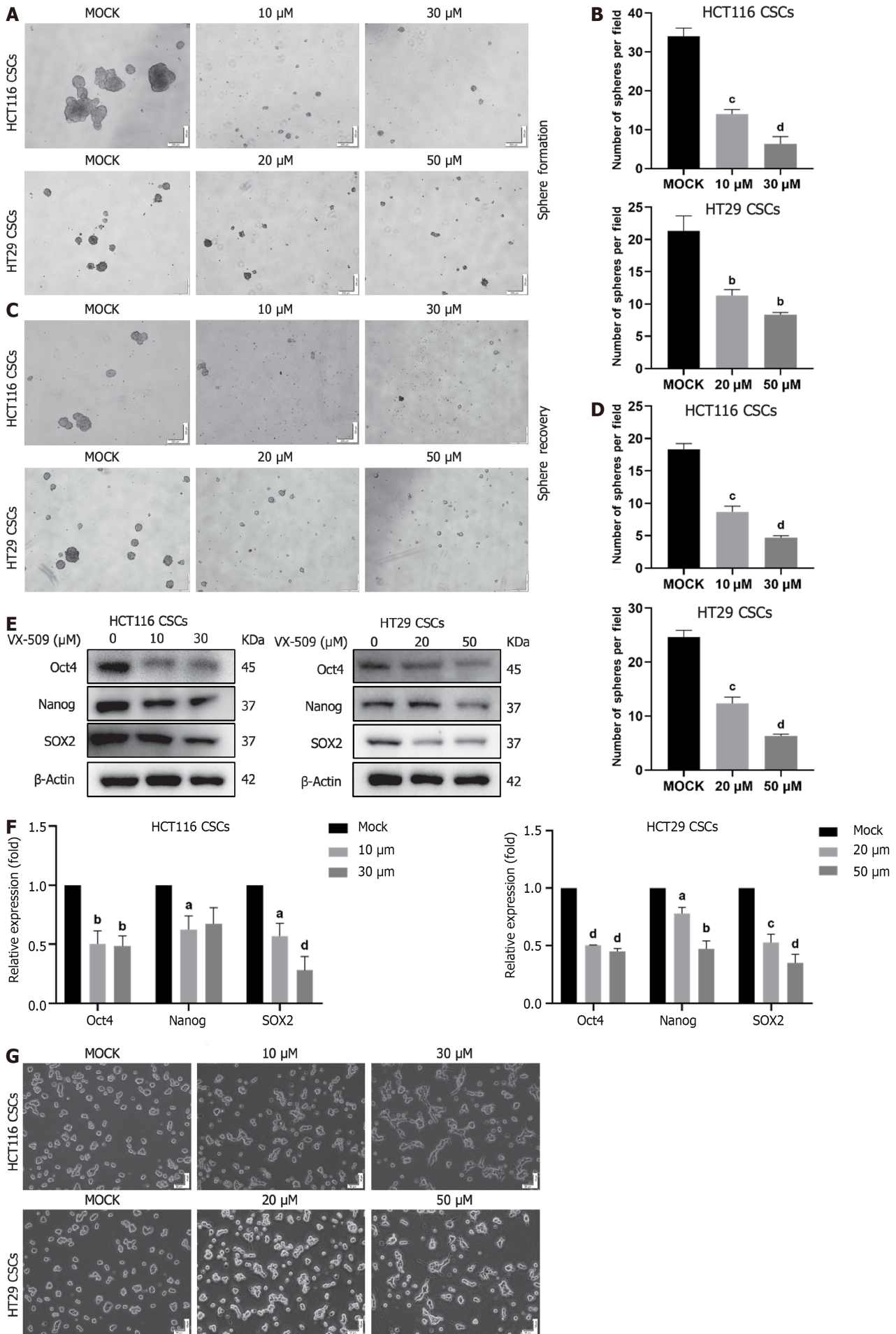
To further explore the effect of VX-509 on the stemness of CCSCs at the time of cell transcription, VX-509-treated HT29 CSCs and control HCT116 CSCs were collected for eukaryotic transcriptome sequencing analysis. Human CSC-related pathway information was downloaded from the MSigDB, and 456 genes related to CSCs were sorted from the 30 lipid metabolism pathways, as shown in Table 1[31]. According to the volcano plot results, 29 differentially expressed genes, including 27 upregulated genes and 2 downregulated genes, were identified (Figure 5A). The expression profiles of all

Table 1 Pathways related to cancer stem cells in Reactome and Gene Ontology databases

Stem cell function related pathways	Pathway ID	Gene count
GO: Somatic stem cell population maintenance	GO: 0035019	72
GO: Negative regulation of stem cell differentiation	GO: 2000737	20
GO: Stem cell proliferation	GO: 0072089	118
GO: Hematopoietic stem cell differentiation	GO: 0060218	79
GO: Negative regulation of stem cell proliferation	GO: 2000647	16
GO: Stem cell division	GO: 0017145	41
GO: Hematopoietic stem cell proliferation	GO: 0071425	23
GO: Positive regulation of stem cell differentiation	GO: 2000738	20
GO: Regulation of stem cell population maintenance	GO: 2000036	28
GO: Neuronal stem cell population maintenance	GO: 0097150	22
GO: Regulation of stem cell proliferation	GO: 0072091	67
GO: Somatic stem cell division	GO: 0048103	24
GO: Stem cell differentiation	GO: 0048863	248
GO: Positive regulation of stem cell proliferation	GO: 2000648	40
GO: Regulation of stem cell differentiation	GO: 2000736	112
GO: Hematopoietic stem cell migration	GO: 0035701	6
GO: Stem cell fate commitment	GO: 0048865	9
GO: Mesenchymal stem cell maintenance involved in nephron morphogenesis	GO: 0072038	6
GO: Mesenchymal stem cell differentiation	GO: 0072497	8
GO: Mesenchymal stem cell proliferation	GO: 0097168	5
GO: Asymmetric stem cell division	GO: 0098722	10
GO: Regulation of hematopoietic stem cell proliferation	GO: 1902033	9
GO: Positive regulation of hematopoietic stem cell proliferation	GO: 1902035	5
GO: Negative regulation of stem cell population maintenance	GO: 1902455	8
GO: Positive regulation of stem cell population maintenance	GO: 1902459	8
GO: Regulation of somatic stem cell population maintenance	GO: 1904672	7
GO: Negative regulation of somatic stem cell population maintenance	GO: 1904673	5
GO: Regulation of stem cell division	GO: 2000035	10
GO: Regulation of mesenchymal stem cell differentiation	GO: 2000739	6
Reactome transcriptional regulation of pluripotent stem cells	R-HSA-452723	31

GO: Gene Ontology.

the genes were analyzed according to the stem cell function related pathways in the GO database (Figure 5B). Nodal was shown to be particularly downregulated and has been demonstrated to be associated with the regulation of stem cell population maintenance. To further confirm the accuracy of the differential sequencing gene analysis, RNA-seq was carried out. After treatment with VX-509, gene expression levels were determined using real-time quantitative polymerase chain reaction, and the results showed that Nodal expression was decreased in HCT116 CSCs and HT29 CSCs compared to control cells (Figure 5C). Smad2 and Smad3 are potent downstream targets of Nodal[32]. As shown in Figure 5D and E, VX-509 treatment significantly reduced the protein expression of Nodal and blocked Smad2 and Smad3 phosphorylation. VX-509 has been reported to be a potent selective JAK3 inhibitor; therefore, we detected the expression of JAK3 in HCT116 CSCs and HT29 CSCs treated with different concentrations of VX-509. The results demonstrated no significant difference in protein expression among the groups (Figure 5F). In conclusion, VX-509 directly downregulated the expression of Nodal to inhibit the phosphorylation of Smad2 and Smad3.



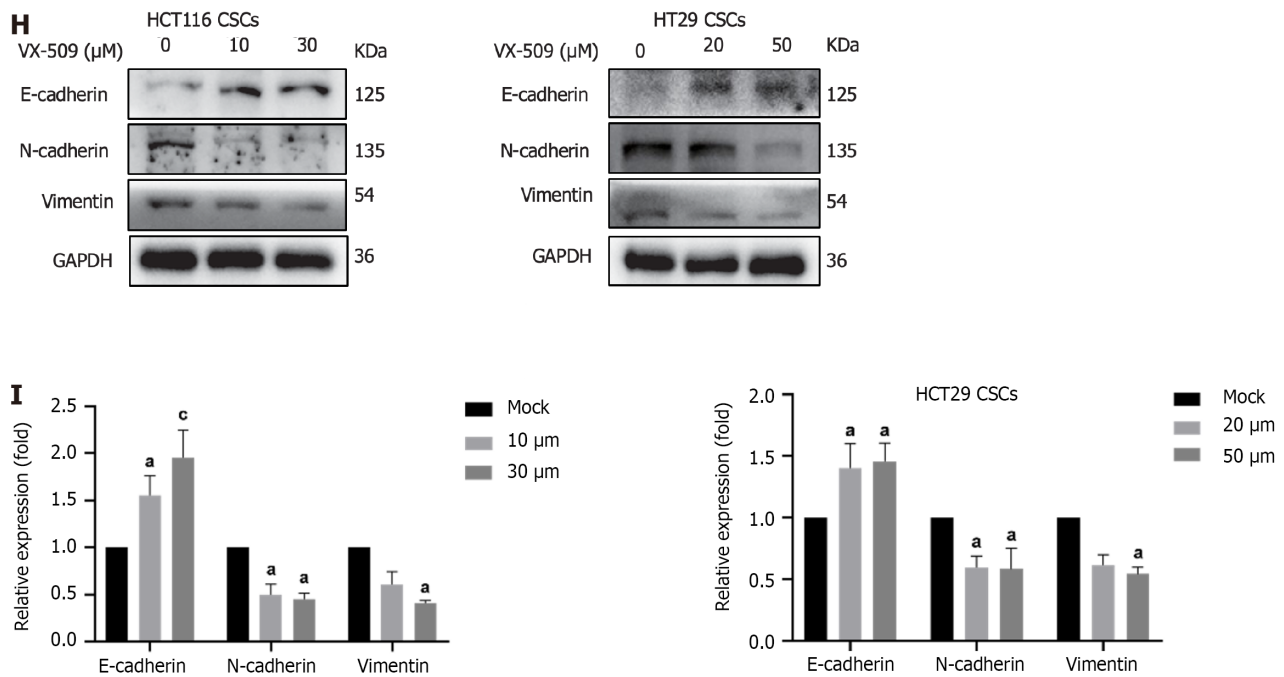


Figure 3 VX-509 inhibits the cancer stem cells characteristics of colorectal cancer-derived cancer stem cells and has an inverse effect on the epithelial-mesenchymal transition progression. A-D: Representative morphology after VX-509 treatment (A, sphere formation assay) or pretreatment (C, sphere recovery assay) and relative statistical analysis (B and D); E: Western blot analysis of Oct4, Nanog, and SOX2 in colorectal cancer (CRC)-derived cancer stem cells (CSCs) treated with different concentrations of VX-509; F: Densitometric analysis of Oct4, Nanog, and SOX2, normalized against β -actin; G: Representative morphology of CRC-derived CSCs in regular 6-well plates after different concentrations of VX-509 treatment; H and I: The effects of different concentrations of VX-509 on the protein expression of E-cadherin, N-cadherin, and vimentin in CRC-derived CSCs were detected by western blot and relative statistical analysis, normalized against GAPDH. Scale bar = 50, 200 μ m. $n = 3$. ^a $P < 0.05$, ^b $P < 0.01$, ^c $P < 0.001$, ^d $P < 0.0001$ compared to the HCT116 cancer stem cells Mock group and HT29 cancer stem cells Mock group. CSC: Cancer stem cell.

VX-509 inhibited the progression of EMT stimulated by Nodal and impeded the dedifferentiation of CCSCs to reduce the stemness of CRC stem-like cells

Nodal, as a precursor protein, is secreted by cells and binds to cell surface receptor complexes to activate related signaling pathways. Exogenous recombinant Nodal protein maintains the spherical morphology of stem cells and enhances the stemness of these cells[15]. As shown in Figure 6A, the cells in the Nodal recombinant protein stimulation group maintained CSC spheres consistent with those of the cells in the control group. However, VX-509 treatment converted sphere CSCs into epithelial-like CRC cells in a Nodal stimulation environment. To observe the effect of Nodal stimulation on EMT, CCSCs were stimulated with Nodal and VX-509 for 24 h, after which the cells were collected for protein detection. As expected, Nodal stimulation reduced the protein expression of E-cadherin and induced the protein expression of N-cadherin and vimentin. VX-509 treatment blocked the Nodal-induced activation of EMT-related proteins in CCSCs (Figure 6B and C). Furthermore, VX-509 treatment significantly suppressed the increase in the protein expression of Nodal and the phosphorylation of Samd2/Samd3 induced by Nodal overexpression (Figure 6D and E). Collectively, our results suggested that VX-509 potentially inhibited Nodal-induced EMT progression by restraining the expression of Nodal.

DISCUSSION

Considering the unsatisfactory therapeutic effects of currently available treatments for CRC, novel and effective methods for diagnosing and prolonging the survival of CRC patients are urgently needed. Numerous studies have demonstrated that a small population of CCSCs isolated from solid tumors in CRC patients possess self-renewal ability and multidirectional differentiation potential[33]. CCSCs are generally in a non-proliferative, static state; however, activated CCSCs exhibit morphological heterogeneity during differentiation, preventing conventional treatments from eliminating these malignant cells. CCSCs are considered important factors leading to the recurrence and metastasis of CRC after treatment. When cultured in SFM supplemented with EGF, bFGF, or other growth factors, differentiated cells cannot proliferate due to intolerance to non-nutrient environments, ultimately resulting in death, while undifferentiated cells survive and revert to stem/progenitor cells[34,35]. The serum-free suspension culture method was used to collect CCSCs in this study. CD133 (prominin-1) upregulates FLICE-like inhibitory protein expression, which is involved in metastasis, metabolism, tumorigenesis, drug resistance, apoptosis and autophagy in CSCs[36]. CD44 is a multi-structural multifunctional transmembrane glycoprotein capable of binding extracellular matrix components to promote cell adhesion as well as cell surface growth factor binding, maintaining interactions between cells and matrix[37]. CD44-positive CSCs perceive

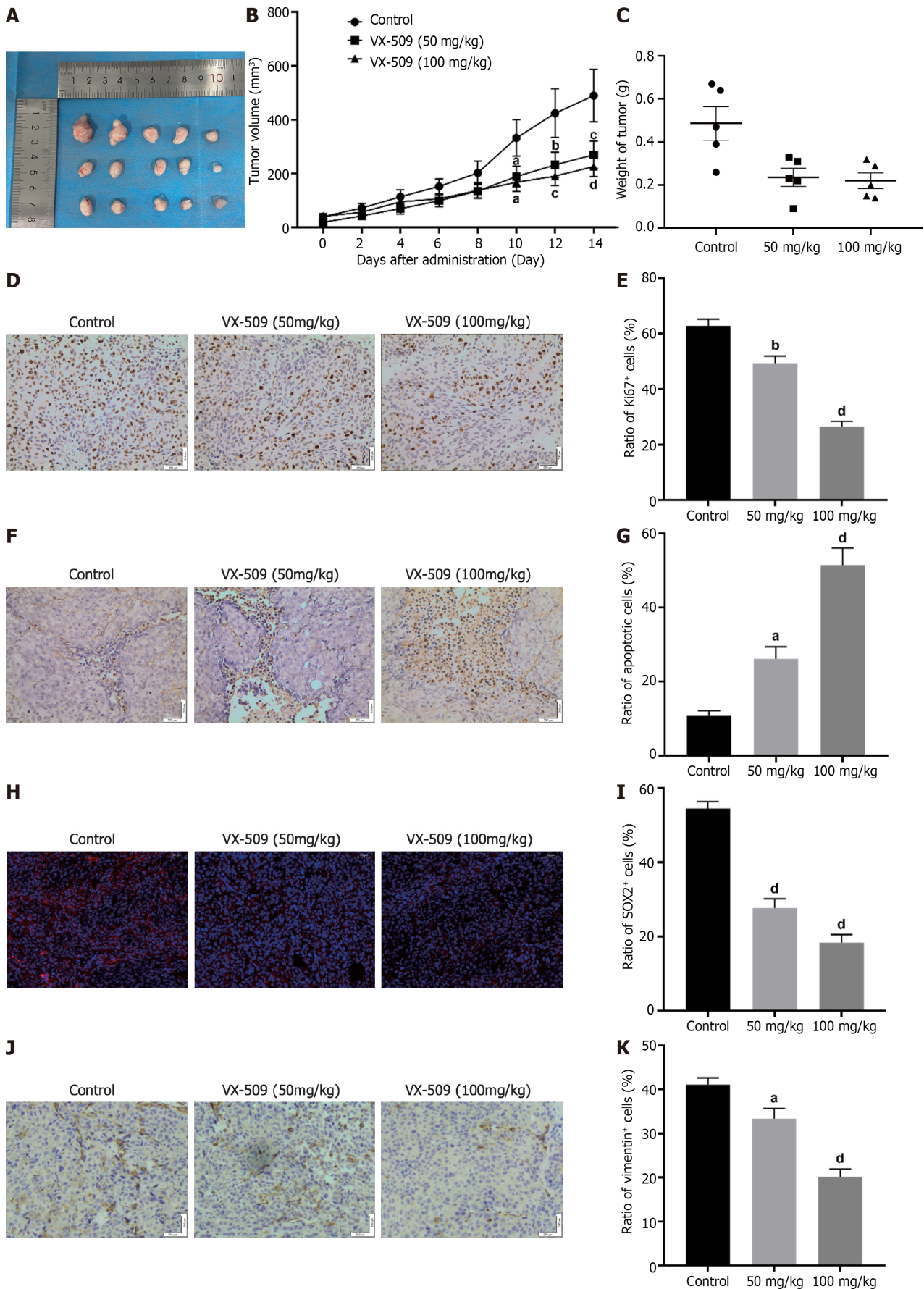


Figure 4 Anticancer efficacy of VX-509 against xenografts derived from colorectal cancer-derived cancer stem cells. A: Tumors derived from HCT116 cancer stem cell (CSC)-bearing nude mice after 14 d of VX-509 treatment; B and C: The statistics of tumor volumes (B) and tumor weights (C) from HCT116 CSC-bearing nude mice treated with VX-509; D-K: Representative immunohistochemical images of Ki67 (D), TUNEL (F) and vimentin (J) as well as the mean of the

IODs of Ki67 (E), TUNEL (G) and vimentin (K) in tumors from HCT116 CSC-bearing nude mice treated with VX-509 are shown. Representative immunofluorescent images of SOX2 (H) as well as the mean of the IOD of SOX2 (I) of tumors from HCT116 CSCs bearing nude mice treated with VX-509 are shown. Scale bars = 50 or 200 μm . $n = 5$. ^a $P < 0.05$, ^b $P < 0.01$, ^c $P < 0.001$, ^d $P < 0.0001$ compared to the control group.

environmental changes that modulate signal transduction, regulating the stemness characteristics of CSCs[38]. Somatic cells can transform into pluripotent stem cells through the transient ectopic overexpression of transcription factors such as Oct4, SOX2, and Nanog, which participate in the regulation CSC self-renewal and development[39]. ALDH1, a cytoplasmic lysozyme, catalyzes the oxidation of the retinol metabolite retinal to retinoic acid and maintains intracellular environmental stability. The expression level of ALDH1 is associated with CCSCs stemness[40]. In this study, SFM-enriched HCT116 CSCs and HT29 CSCs were collected, and the expression levels of CD133, CD44, Oct4, SOX2, Nanog and ALDH were detected. The results revealed that, compared with parental cells, sphere cells exhibited higher expression levels of cell surface markers and transcription factors. Additionally, cell migration experiments demonstrated that sphere cells displayed greater migratory capacity than parental cells. *In vivo* tumorigenesis experiments revealed that the sphere cells were approximately 10-fold more tumorigenic than the parental cells were. Based on these experimental findings, it was preliminarily confirmed that HCT116 CSCs and HT29 CCSCs were successfully constructed.

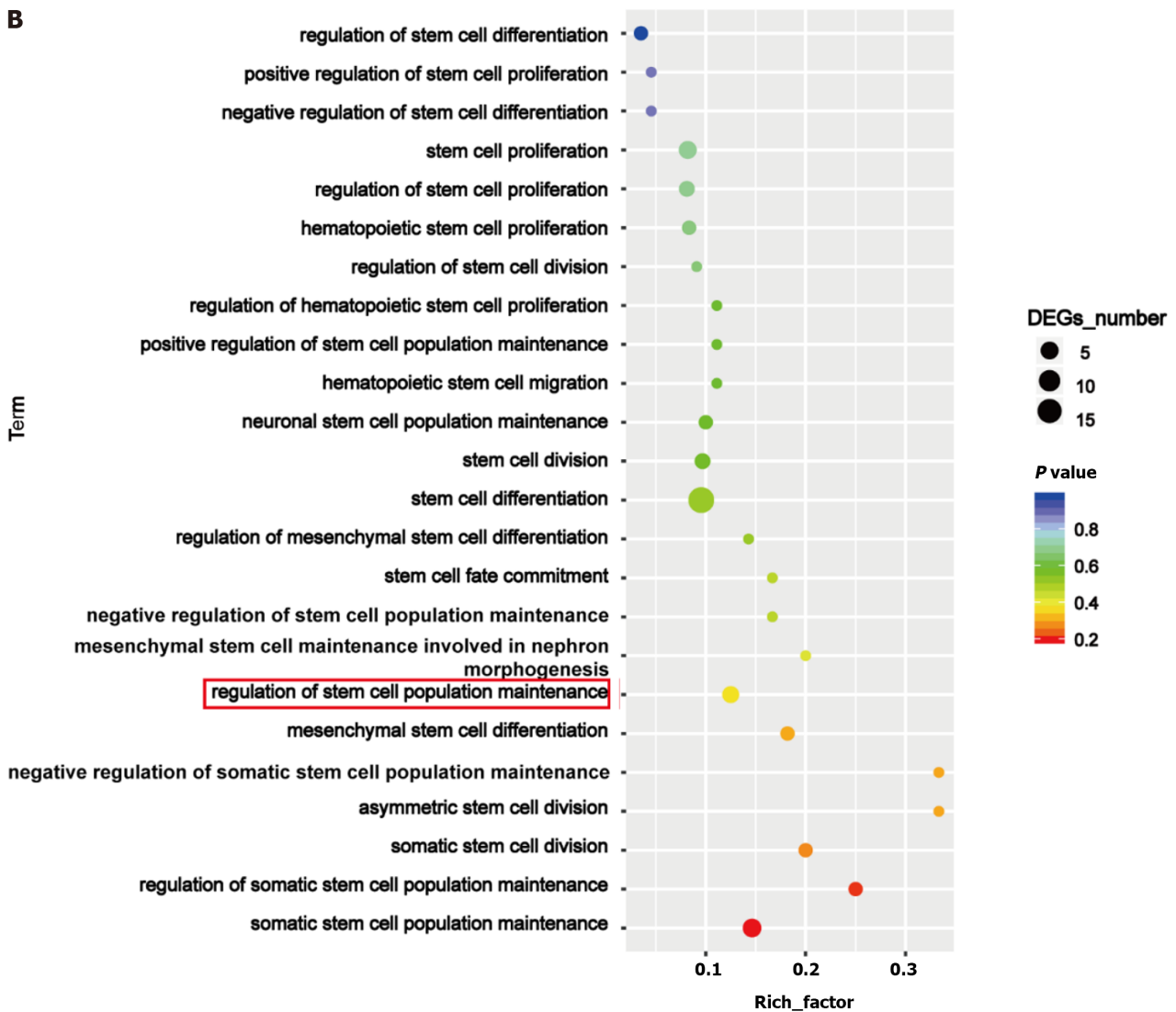
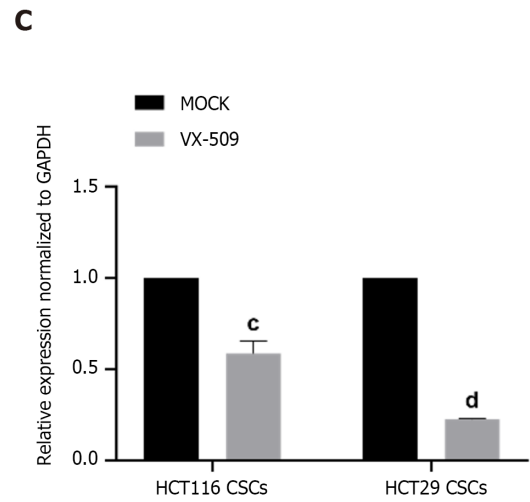
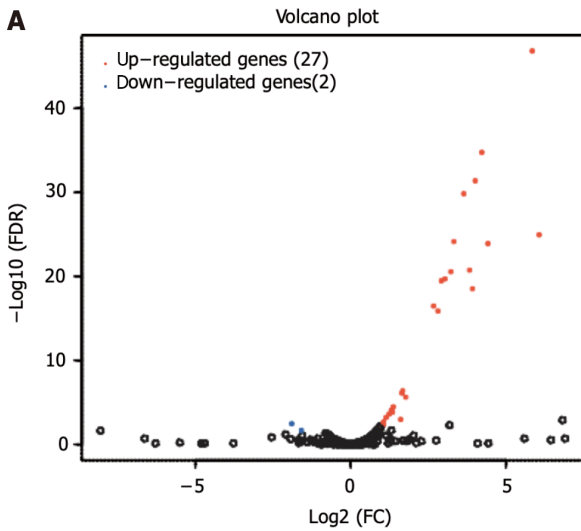
VX-509, as a selective JAK3 inhibitor, has been reported to be a potent treatment for RA[41]. Mahajan *et al*[18] discovered that VX-509 effectively alleviated ankle swelling in collagen-induced RA mice by inhibiting JAK3 protein expression. Furthermore, clinical studies have shown that VX-509 combined with the common nonsteroidal drug methotrexate can significantly improve joint swelling and tenderness in RA patients[42]. VX-509 served as a conventional drug for treating RA. In our previous study, we used a small-molecule compound inhibitor library to identify inhibitors with potent activity against the stemness of CCSCs, and VX-509 exhibited stemness inhibitory effects from the obvious morphological changes in spherical cancer stem cells to epithelial adherent cancer cells. As VX-509 inhibits JAK3, the expression of the JAK3 protein in CCSCs after VX-509 treatment was assessed, and no significant difference was detected among the groups (Figure 5F). EMT is a dynamic and reversible process wherein epithelial cells transform into the mesenchymal cells through the induction of multiple factors[43]. In response to external stimuli, EMT is reversed, and mesenchymal cells transform into epithelial cells[44], which is consistent with our morphological alteration results. Therefore, we explored the effect of VX-509 on EMT-related signaling rather than JAK3 signaling.

Self-renewal and malignant differentiation are the main factors leading to poor prognosis in CRC patients; therefore, we aimed to eradicate CCSCs by preventing their generation and continuous dedifferentiation. We used different drugs to stimulate CCSC dedifferentiation *via* growth factors and observed morphological changes by microscopy to identify effective drugs for CCSCs dedifferentiation. Additionally, CCK-8 assay was performed to evaluate changes in cell viability upon exposure to various concentrations of the candidate drugs (Figure 2A). We found that VX-509 inhibited the dedifferentiation of CCSCs and inhibited cell viability in a dose-dependent manner. Therefore, VX-509 was selected for subsequent studies.

Continuous proliferation is a fundamental characteristic of malignant tumors. In the present study, VX-509 significantly suppressed the proliferation process and induced apoptosis in CCSCs (Figure 2B-E). Malignant tumor cells possess strong migratory abilities, enabling them to seek alternative energy sources within the human body; thus, migration serves as an important manifestation of their malignant biological characteristics. Our results demonstrated that VX-509 effectively suppressed the migratory capacity of CCSCs (Figure 2F). In addition, VX-509 significantly inhibited the clonogenicity of CCSCs (Figure 2H). *In vivo* experiments revealed that VX-509 treatment dose-dependently suppressed tumor growth in HCT116-derived CSC-bearing nude mice and induced increased apoptosis (Figure 4A). Sphere formation is an important feature of the self-renewal ability of cancer stem cells. Different concentrations of VX-509 significantly inhibited the sphere formation rate of CCSCs (Figure 3A). Additionally, protein analysis further confirmed that VX-509 downregulated the expression of relevant transcription factors (Figure 3E). Similarly, treatment with VX-509 dramatically reduced the proportion of SOX2-positive cells in HCT116 CSC-derived xenografts (Figure 4H). Taken together, our findings confirmed the inhibitory effect of VX-509 on the stemness of CCSCs according to phenotype.

The EMT plays crucial roles in both physiological and pathological processes, including tumor development[45]. The EMT endows tumor cells with extreme plasticity, which promotes tumor cell diversity and intracellular heterogeneity. Moreover, cell plasticity regulates the dynamic transition between tumor cells with limited tumorigenic potential in the differentiated state and CSCs with indeterminate growth in the undifferentiated state[46]. Therefore, EMT serves as an important origin of cancer development. In our study, treatment with VX-509 induced the differentiation of compact spheres derived from CCSCs into adherent epithelioid tumor cells (Figure 3G). Considering the distinct inhibitory effect of VX-509 on the migration of CCSCs, we speculated that the mechanism underlying its stemness inhibition may be closely associated with EMT regulation. The results of the EMT phenotype protein analysis confirmed our speculation that VX-509 treatment inhibited the EMT process in CCSCs (Figure 3H). Similarly, VX-509 treatment dramatically reduced the proportion of vimentin-positive cells in HCT116 CSC-derived xenografts (Figure 4J). Overall, we proposed that VX-509 prevents the dedifferentiation and stemness of CCSCs by regulating the EMT process.

Nodal, a member of the TGF- β superfamily, is crucial for the proliferation of human and mouse embryonic stem cells [47]. Nodal binds to serine-threonine kinase receptor complexes (ALK4/7, ACTRIIA and ACTRIIB) on the polarized surfaces of cells. The glycosyl phosphatidylinositol-linked coreceptors of the epidermal growth factor-Cripto-FRL-Criptin (EGF-CFC) family members teratocancer-derived growth factor 1 and Cripto1 are involved in Nodal signaling[48]. Upon activation, Nodal phosphorylates Smad2/3 receptors, which then form complexes with Smad4 and accumulate in the cell nucleus to regulate related transcriptional processes[49]. In addition to its essential role in embryogenesis, Nodal also plays significant role in cancer development and metastasis. Previous studies have reported that Nodal induced the



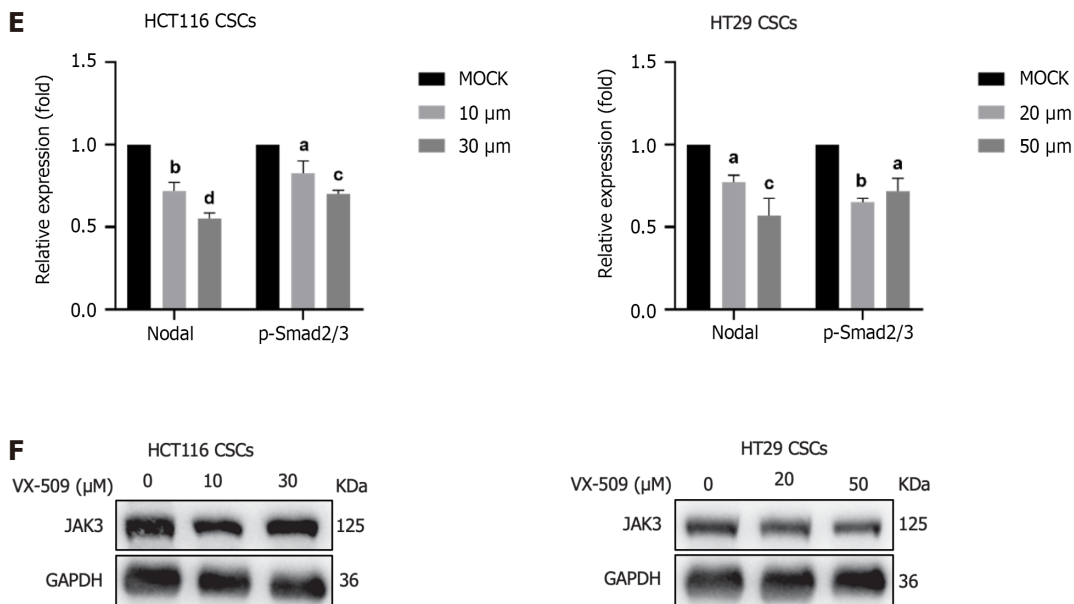


Figure 5 VX-509 downregulates Nodal and its downstream protein p-Smad2/3 in colorectal cancer-derived cancer stem cells. A: Volcano plot of differentially expressed genes in the HT29 cancer stem cells (CSCs) Mock and VX-509-treated groups; B: Gene Ontology enrichment image of the differentially expressed genes; C: Nodal mRNA expression levels in the colorectal cancer (CRC)-derived CSCs Mock and VX-509-treated group; D-F: Protein expression levels of Nodal, p-Smad2/3 (D) and JAK3 (F) in CRC-derived CSCs treated with different concentrations of VX-509 (E). Densitometric analysis of Nodal and p-Smad2/3, normalized against GAPDH. $n = 3$. ^a $P < 0.05$, ^b $P < 0.01$, ^c $P < 0.001$, ^d $P < 0.0001$ compared to the HCT116 cancer stem cells Mock group and HT29 cancer stem cells Mock group. CSC: Cancer stem cell; DEG: Differentially expressed gene.

metastatic phenotype of pancreatic cancer cells through the Smad2/3 phosphorylation pathway[50]. In this study, we used the DEGs and information retrieved from a CSC-related database to confirm that Nodal was the regulatory gene involved (Figure 5A and B). Furthermore, protein experiments confirmed that VX-509 significantly inhibited both the expression of Nodal and the phosphorylation of Smad2/3, its downstream effector protein (Figure 5D).

Exogenous recombinant protein stimulation activates signaling pathways in cells to upregulate the expression of related proteins, which can be used to verify the direct relationship between drugs and regulatory proteins. Recent research revealed that the exogenous addition of recombinant Nodal protein (20 ng/mL) promoted the formation of CCSC spheroids and increased the phosphorylation of Smad2/3, which indicated that Nodal is involved in the self-renewal process of CCSCs[15]. In our experiment, compared with the control treatment, Nodal stimulation led to pronounced aggregation of CCSCs into spheres. However, treatment with an effective dose of VX-509 inhibited this phenomenon and induced the cells to attach and stretch into epithelioid tumor cells (Figure 6A). Additionally, protein analysis demonstrated that the expression of EMT proteins in CCSCs was increased in the Nodal-stimulated group (Figure 6B), suggesting that Nodal induces the EMT process in CCSCs. These findings provide a more robust theoretical foundation for understanding the involvement of Nodal in regulating the stem-like properties of CCSCs. Treatment with VX-509 suppressed EMT-related phenotypic proteins, suggesting its ability to reverse activation induced by Nodal stimulation and inhibit the dedifferentiation process in CCSCs.

CONCLUSION

In this study, we utilized SFM enriched with growth factors to isolate CCSCs derived from the human CRC cell lines HCT116 and HT29, confirming their stemness characteristics compared to parental tumor cells. A small-molecule inhibitor library was subsequently used to screen VX-509, a drug that exhibited significant inhibitory effects on dedifferentiation processes in CCSCs. Malignant biological behavior experiments further confirmed that VX-509 could prevent malignant proliferation, promote apoptosis, prevent invasion and metastasis, and inhibit tumor aggregation within CCSCs. Moreover, VX-509 regulated the transcription and protein expression of Nodal and inhibited the phosphorylation of the downstream protein Smad2/3 to prevent the EMT process in CCSCs, inhibited the continuous self-renewal of CCSCs and consequently reduced the generation of CCSCs, suggesting its potential clinical application in treating CRC.

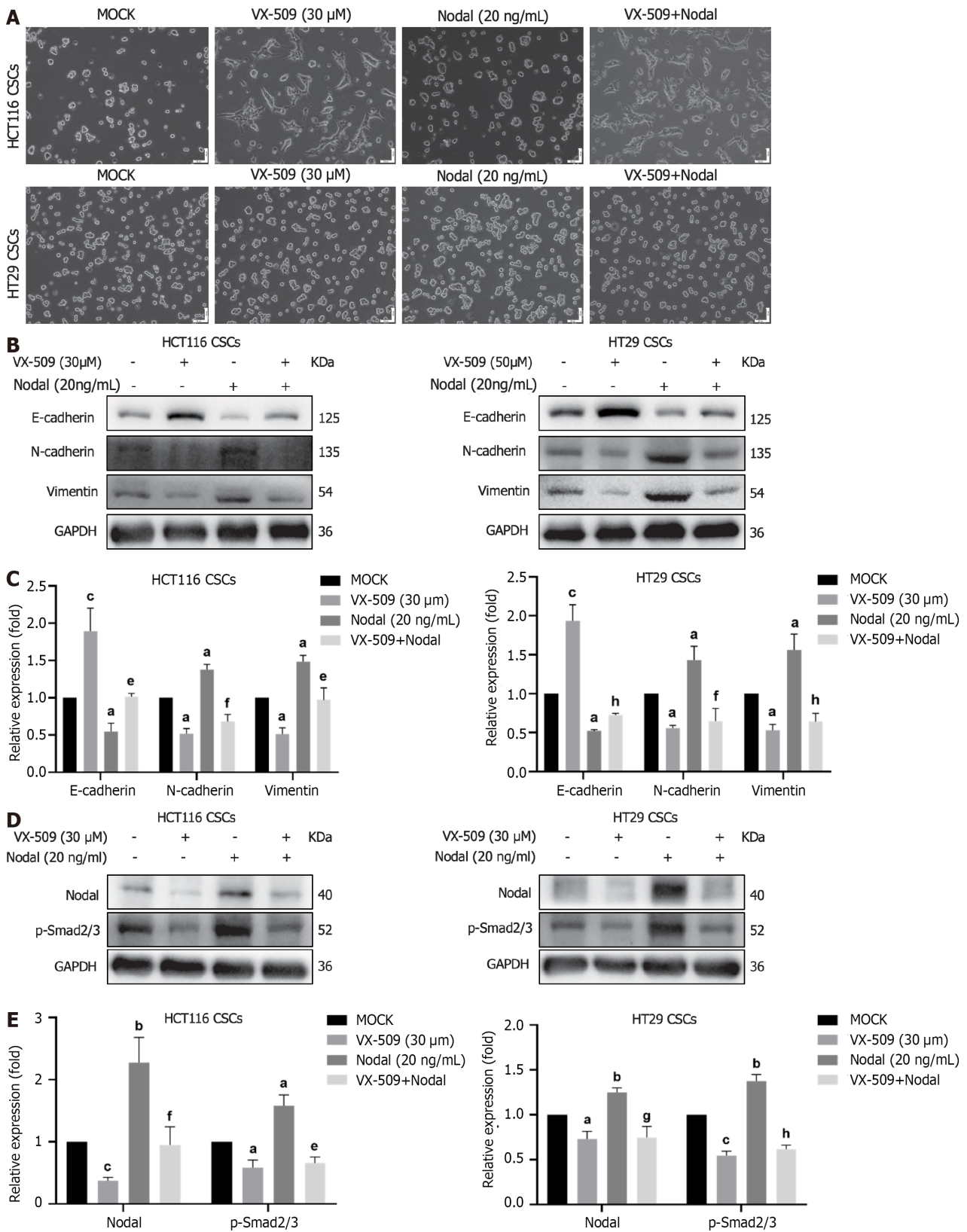


Figure 6 VX-509 reverses the increase in epithelial-mesenchymal transition progression induced by Nodal over expression in colorectal cancer-derived cancer stem cells. **A:** Morphological changes in Nodal-stimulated colorectal cancer (CRC)-derived cancer stem cells (CSCs) treated with different concentrations of VX-509 observed *via* microscopy; **B and C:** The effects of VX-509 on the protein expression levels of E-cadherin, N-cadherin, and vimentin in Nodal-stimulated CRC-derived CSCs were detected by western blot and relative statistical analysis, normalized against GAPDH; **D and E:** The effects of VX-509 on the protein expression levels of Nodal and p-Smad2/3 in Nodal-stimulated CRC-derived CSCs were detected by western blot and relative statistical analysis, normalized against GAPDH. *n* = 3. ^a*P* < 0.05, ^b*P* < 0.001, ^c*P* < 0.05 compared to the HCT116 cancer stem cells Mock group and HT29 cancer stem cells Mock group. ^f*P* < 0.05, ^g*P* < 0.01, ^h*P* < 0.0001 compared to the HCT116 cancer stem cells Nodal group and HT29 CSCs Nodal group.

ARTICLE HIGHLIGHTS

Research background

Colorectal cancer (CRC) is a globally prevalent malignant disease with a significant increase in incidence, and CRC patients continue to face poor outcomes characterized by ineffective early-stage diagnosis, recurrence and metastasis due to incomplete tumor removal, and resistance to chemoradiotherapy.

Research motivation

Colorectal cancer stem cells (CCSCs), that possess self-renewal ability and the capacity for multidirectional differentiation, strongly support disordered tumor growth and treatment resistance. Targeting CCSCs can be an effective strategy for eradicating CRC from the source.

Research objectives

The present study aimed to investigate the effect of VX-509 on CCSCs and elucidate the underlying mechanism.

Research methods

CCSCs were enriched from CRC cell lines and were verified the cancer stem-like phenotypic characteristics. The anticancer efficacy of VX-509 was assessed in HCT116 CCSCs and HT29 CCSCs by performing cell viability analysis, colony formation, sphere formation, flow cytometry, and western blotting assessments *in vitro* and tumor growth, immunohistochemistry and immunofluorescence assessments *in vivo*.

Research results

HCT116 CCSCs and HT29 CCSCs were enriched successfully and possessed CCSC characteristics. VX-509 inhibited the tumor malignant biological behaviors and the CSC characteristics of CCSCs. Besides, VX-509 suppressed the progression of epithelial-mesenchymal transition (EMT) signaling and downregulated the expression of Nodal and its downstream phosphorylated Smad2/3.

Research conclusions

This study demonstrated that VX-509 prevents the EMT process in CCSCs by inhibiting the transcription and protein expression of Nodal, and inhibits the dedifferentiated self-renewal of CCSCs.

Research perspectives

VX-509 inhibited the continuous self-renewal and reduced the generation of CCSCs by regulating the transcription and protein expression of Nodal to inhibit the EMT process, suggesting its potential clinical application in treating CRC.

FOOTNOTES

Co-first authors: Yun Yuan and Xu-Fan Zhang.

Co-corresponding authors: Jia-Lian Zheng and Qiong-Ying Hu.

Author contributions: Yuan Y, Zhang XF, Li YC, Chen HQ, Wen T, Zheng JL, Zhao ZY, and Hu QY contributed to the investigation of this manuscript; Yuan Y, Li YC, Chen HQ, and Wen T were involved in the data curation; Yuan Y, Li YC, Zheng JL, and Hu QY participated in the methodology of this study; Yuan Y, Zhang XF, Zheng JL, Zhao ZY, and Hu QY took part in the conceptualization of this article; Yuan Y and Zhang XF wrote the original draft; Zhang XF, Zheng JL, and Hu QY contributed to the project administration of this manuscript; Zheng JL, Zhao ZY, and Hu QY were major in the funding acquisition and supervision of this program.

Supported by National Natural Science Foundation of China, No. 82074298; Chengdu Science and Technology Bureau Project, No. 2021-YF05-01726-SN; and “Xinglin Scholars” Research Promotion Program of Chengdu University of Traditional Chinese Medicine, No. QJRC2022007.

Institutional review board statement: The study was reviewed and approved by Related Ethical Regulations of Chengdu University of Traditional Chinese Medicine.

Institutional animal care and use committee statement: All the animal experiments were approved by the ethics committee of the Institutional Animal Care and Use Committee of Institute of Chengdu University of Traditional Chinese Medicine.

Conflict-of-interest statement: All the authors report no relevant conflicts of interest for this article.

Data sharing statement: All data during the study are available from the corresponding author by request at qiongyinghu@163.com.

ARRIVE guidelines statement: The authors have read the ARRIVE guidelines, and the manuscript was prepared and revised according to the ARRIVE guidelines.

Open-Access: This article is an open-access article that was selected by an in-house editor and fully peer-reviewed by external reviewers. It is distributed in accordance with the Creative Commons Attribution NonCommercial (CC BY-NC 4.0) license, which permits others to distribute, remix, adapt, build upon this work non-commercially, and license their derivative works on different terms, provided the original work is properly cited and the use is non-commercial. See: <https://creativecommons.org/licenses/by-nc/4.0/>

Country/Territory of origin: China

ORCID number: Yun Yuan 0009-0006-9100-9482; Jia-Lian Zheng 0009-0005-0438-5141; Zi-Yi Zhao 0000-0003-1871-5197; Qiong-Ying Hu 0000-0002-1718-4542.

S-Editor: Wang JJ

L-Editor: A

P-Editor: Zhang XD

REFERENCES

- Sung H, Ferlay J, Siegel RL, Laversanne M, Soerjomataram I, Jemal A, Bray F. Global Cancer Statistics 2020: GLOBOCAN Estimates of Incidence and Mortality Worldwide for 36 Cancers in 185 Countries. *CA Cancer J Clin* 2021; **71**: 209-249 [PMID: 33538338 DOI: 10.3322/caac.21660]
- Morgan E, Arnold M, Gini A, Lorenzoni V, Cabaasag CJ, Laversanne M, Vignat J, Ferlay J, Murphy N, Bray F. Global burden of colorectal cancer in 2020 and 2040: incidence and mortality estimates from GLOBOCAN. *Gut* 2023; **72**: 338-344 [PMID: 36604116 DOI: 10.1136/gutjnl-2022-327736]
- Sawicki T, Ruzkowska M, Danielewicz A, Niedźwiedzka E, Arłukowicz T, Przybyłowicz KE. A Review of Colorectal Cancer in Terms of Epidemiology, Risk Factors, Development, Symptoms and Diagnosis. *Cancers (Basel)* 2021; **13** [PMID: 33922197 DOI: 10.3390/cancers13092025]
- Han J, Won M, Kim JH, Jung E, Min K, Jangili P, Kim JS. Cancer stem cell-targeted bio-imaging and chemotherapeutic perspective. *Chem Soc Rev* 2020; **49**: 7856-7878 [PMID: 32633291 DOI: 10.1039/d0cs00379d]
- Jahanafrooz Z, Mosafer J, Akbari M, Hashemzaei M, Mokhtarzadeh A, Baradaran B. Colon cancer therapy by focusing on colon cancer stem cells and their tumor microenvironment. *J Cell Physiol* 2020; **235**: 4153-4166 [PMID: 31647128 DOI: 10.1002/jcp.29337]
- Lüönd F, Tiede S, Christofori G. Breast cancer as an example of tumour heterogeneity and tumour cell plasticity during malignant progression. *Br J Cancer* 2021; **125**: 164-175 [PMID: 33824479 DOI: 10.1038/s41416-021-01328-7]
- O'Brien CA, Pollett A, Gallinger S, Dick JE. A human colon cancer cell capable of initiating tumour growth in immunodeficient mice. *Nature* 2007; **445**: 106-110 [PMID: 17122772 DOI: 10.1038/nature05372]
- Schwitalla S, Fingerle AA, Cammareri P, Nebelsiek T, Göktuna SI, Ziegler PK, Canli O, Heijmans J, Huels DJ, Moreaux G, Rupec RA, Gerhard M, Schmid R, Barker N, Clevers H, Lang R, Neumann J, Kirchner T, Taketo MM, van den Brink GR, Sansom OJ, Arkan MC, Greten FR. Intestinal tumorigenesis initiated by dedifferentiation and acquisition of stem-cell-like properties. *Cell* 2013; **152**: 25-38 [PMID: 23273993 DOI: 10.1016/j.cell.2012.12.012]
- Babaei G, Aziz SG, Jaghi NZZ. EMT, cancer stem cells and autophagy; The three main axes of metastasis. *Biomed Pharmacother* 2021; **133**: 110909 [PMID: 33227701 DOI: 10.1016/j.biopha.2020.110909]
- Wilson MM, Weinberg RA, Lees JA, Guen VJ. Emerging Mechanisms by which EMT Programs Control Stemness. *Trends Cancer* 2020; **6**: 775-780 [PMID: 32312682 DOI: 10.1016/j.trecan.2020.03.011]
- Cui Y, Zhao M, Yang Y, Xu R, Tong L, Liang J, Zhang X, Sun Y, Fan Y. Reversal of epithelial-mesenchymal transition and inhibition of tumor stemness of breast cancer cells through advanced combined chemotherapy. *Acta Biomater* 2022; **152**: 380-392 [PMID: 36028199 DOI: 10.1016/j.actbio.2022.08.024]
- Zhu Y, Wang C, Becker SA, Hurst K, Nogueira LM, Findlay VJ, Camp ER. miR-145 Antagonizes SNAIL-Mediated Stemness and Radiation Resistance in Colorectal Cancer. *Mol Ther* 2018; **26**: 744-754 [PMID: 29475734 DOI: 10.1016/j.ymthe.2017.12.023]
- Lord ND, Carte AN, Abitua PB, Schier AF. The pattern of nodal morphogen signaling is shaped by co-receptor expression. *Elife* 2021; **10** [PMID: 34036935 DOI: 10.7554/eLife.54894]
- Quail DF, Zhang G, Findlay SD, Hess DA, Postovit LM. Nodal promotes invasive phenotypes via a mitogen-activated protein kinase-dependent pathway. *Oncogene* 2014; **33**: 461-473 [PMID: 23334323 DOI: 10.1038/onc.2012.608]
- Gong Y, Guo Y, Hai Y, Yang H, Liu Y, Yang S, Zhang Z, Ma M, Liu L, Li Z, He Z. Nodal promotes the self-renewal of human colon cancer stem cells via an autocrine manner through Smad2/3 signaling pathway. *Biomed Res Int* 2014; **2014**: 364134 [PMID: 24696849 DOI: 10.1155/2014/364134]
- Robinette ML, Cella M, Telliez JB, Ulland TK, Barrow AD, Capuder K, Gilfillan S, Lin LL, Notarangelo LD, Colonna M. Jak3 deficiency blocks innate lymphoid cell development. *Mucosal Immunol* 2018; **11**: 50-60 [PMID: 28513593 DOI: 10.1038/mi.2017.38]
- Elwood F, Witter DJ, Piesvaux J, Kraybill B, Bays N, Alpert C, Goldenblatt P, Qu Y, Ivanovska I, Lee HH, Chiu CS, Tang H, Scott ME, Deshmukh SV, Zielstorff M, Byford A, Chakravarthy K, Dorosh L, Rivkin A, Klappenbach J, Pan BS, Kariv I, Dinsmore C, Slipetz D, Dandliker PJ. Evaluation of JAK3 Biology in Autoimmune Disease Using a Highly Selective, Irreversible JAK3 Inhibitor. *J Pharmacol Exp Ther* 2017; **361**: 229-244 [PMID: 28193636 DOI: 10.1124/jpet.116.239723]
- Mahajan S, Hogan JK, Shlyakhter D, Oh L, Salituro FG, Farmer L, Hoock TC. VX-509 (decernotinib) is a potent and selective janus kinase 3 inhibitor that attenuates inflammation in animal models of autoimmune disease. *J Pharmacol Exp Ther* 2015; **353**: 405-414 [PMID: 25762693 DOI: 10.1124/jpet.114.221176]
- Genovese MC, Yang F, Østergaard M, Kinnman N. Efficacy of VX-509 (decernotinib) in combination with a disease-modifying antirheumatic drug in patients with rheumatoid arthritis: clinical and MRI findings. *Ann Rheum Dis* 2016; **75**: 1979-1983 [PMID: 27084959 DOI: 10.1136/annrheumdis-2015-208901]
- Wu T, Yu J, Wang C, Jin Y, Zheng X, Chen L, Ma X, Sun X. Novel Potent EGFR-JAK3 Dual-Target Inhibitor that Overcomes KRAS

- Mutation Resistance in Colorectal Cancer. *Anticancer Agents Med Chem* 2023; **23**: 440-449 [PMID: 35692150 DOI: 10.2174/1871520622666220609112816]
- 21 **Saini MK**, Vaish V, Sanyal SN. Role of cytokines and Jak3/Stat3 signaling in the 1,2-dimethylhydrazine dihydrochloride-induced rat model of colon carcinogenesis: early target in the anticancer strategy. *Eur J Cancer Prev* 2013; **22**: 215-228 [PMID: 23514809 DOI: 10.1097/CEJ.0b013e3283584932]
- 22 **Lin Q**, Lai R, Chiriac LR, Li C, Thomazy VA, Grammatikakis I, Rassidakis GZ, Zhang W, Fujio Y, Kunisada K, Hamilton SR, Amin HM. Constitutive activation of JAK3/STAT3 in colon carcinoma tumors and cell lines: inhibition of JAK3/STAT3 signaling induces apoptosis and cell cycle arrest of colon carcinoma cells. *Am J Pathol* 2005; **167**: 969-980 [PMID: 16192633 DOI: 10.1016/S0002-9440(10)61187-X]
- 23 **Zheng YG**, Wang JA, Meng L, Pei X, Zhang L, An L, Li CL, Miao YL. Design, synthesis, biological activity evaluation of 3-(4-phenyl-1H-imidazol-2-yl)-1H-pyrazole derivatives as potent JAK 2/3 and aurora A/B kinases multi-targeted inhibitors. *Eur J Med Chem* 2021; **209**: 112934 [PMID: 33109396 DOI: 10.1016/j.ejmech.2020.112934]
- 24 **Zhao Z**, Zeng J, Guo Q, Pu K, Yang Y, Chen N, Zhang G, Zhao M, Zheng Q, Tang J, Hu Q. Berberine Suppresses Stemness and Tumorigenicity of Colorectal Cancer Stem-Like Cells by Inhibiting m(6)A Methylation. *Front Oncol* 2021; **11**: 775418 [PMID: 34869024 DOI: 10.3389/fonc.2021.775418]
- 25 **Huang EH**, Hynes MJ, Zhang T, Ginestier C, Dontu G, Appelman H, Fields JZ, Wicha MS, Boman BM. Aldehyde dehydrogenase 1 is a marker for normal and malignant human colonic stem cells (SC) and tracks SC overpopulation during colon tumorigenesis. *Cancer Res* 2009; **69**: 3382-3389 [PMID: 19336570 DOI: 10.1158/0008-5472.CAN-08-4418]
- 26 **Douville J**, Beaulieu R, Balicki D. ALDH1 as a functional marker of cancer stem and progenitor cells. *Stem Cells Dev* 2009; **18**: 17-25 [PMID: 18573038 DOI: 10.1089/scd.2008.0055]
- 27 **Feng H**, Liu Y, Bian X, Zhou F. ALDH1A3 affects colon cancer in vitro proliferation and invasion depending on CXCR4 status. *Br J Cancer* 2018; **118**: 224-232 [PMID: 29235568 DOI: 10.1038/bjc.2017.363]
- 28 **Prabhu VV**, Allen JE, Dicker DT, El-Deiry WS. Small-Molecule ONC201/TIC10 Targets Chemotherapy-Resistant Colorectal Cancer Stem-like Cells in an Akt/Foxo3a/TRAIL-Dependent Manner. *Cancer Res* 2015; **75**: 1423-1432 [PMID: 25712124 DOI: 10.1158/0008-5472.CAN-13-3451]
- 29 **Mather JP**. In vitro models. *Stem Cells* 2012; **30**: 95-99 [PMID: 22076915 DOI: 10.1002/stem.774]
- 30 **Roy S**, Sunkara RR, Parmar MY, Shaikh S, Waghmare SK. EMT imparts cancer stemness and plasticity: new perspectives and therapeutic potential. *Front Biosci (Landmark Ed)* 2021; **26**: 238-265 [PMID: 33049669 DOI: 10.2741/4893]
- 31 **Liang Y**, Su Q, Wu X. Identification and Validation of a Novel Six-Gene Prognostic Signature of Stem Cell Characteristic in Colon Cancer. *Front Oncol* 2020; **10**: 571655 [PMID: 33680915 DOI: 10.3389/fonc.2020.571655]
- 32 **Wei X**, Guo J, Li Q, Jia Q, Jing Q, Li Y, Zhou B, Chen J, Gao S, Zhang X, Jia M, Niu C, Yang W, Zhi X, Wang X, Yu D, Bai L, Wang L, Na J, Zou Y, Zhang J, Zhang S, Meng D. Bach1 regulates self-renewal and impedes mesodermal differentiation of human embryonic stem cells. *Sci Adv* 2019; **5**: eaau7887 [PMID: 30891497 DOI: 10.1126/sciadv.aau7887]
- 33 **Du L**, Cheng Q, Zheng H, Liu J, Liu L, Chen Q. Targeting stemness of cancer stem cells to fight colorectal cancers. *Semin Cancer Biol* 2022; **82**: 150-161 [PMID: 33631296 DOI: 10.1016/j.semcancer.2021.02.012]
- 34 **Hu C**, Li M, Guo T, Wang S, Huang W, Yang K, Liao Z, Wang J, Zhang F, Wang H. Anti-metastasis activity of curcumin against breast cancer via the inhibition of stem cell-like properties and EMT. *Phytomedicine* 2019; **58**: 152740 [PMID: 31005718 DOI: 10.1016/j.phymed.2018.11.001]
- 35 **Nagasaki K**, Nakashima A, Tamura R, Ishiuchi N, Honda K, Ueno T, Doi S, Kato Y, Masaki T. Mesenchymal stem cells cultured in serum-free medium ameliorate experimental peritoneal fibrosis. *Stem Cell Res Ther* 2021; **12**: 203 [PMID: 33757592 DOI: 10.1186/s13287-021-02273-1]
- 36 **Barzegar Behrooz A**, Syahir A, Ahmad S. CD133: beyond a cancer stem cell biomarker. *J Drug Target* 2019; **27**: 257-269 [PMID: 29911902 DOI: 10.1080/1061186X.2018.1479756]
- 37 **Trouvilliez S**, Cicero J, Lévêque R, Aubert L, Corbet C, Van Outryve A, Streule K, Angrand PO, Völkel P, Magnez R, Brysbaert G, Mysiorek C, Gosselet F, Bourette R, Adriaenssens E, Thuru X, Lagade C, de Ruyck J, Orian-Rousseau V, Le Bourhis X, Toillon RA. Direct interaction of TrkA/CD44v3 is essential for NGF-promoted aggressiveness of breast cancer cells. *J Exp Clin Cancer Res* 2022; **41**: 110 [PMID: 35346305 DOI: 10.1186/s13046-022-02314-4]
- 38 **Peng L**, Xiong Y, Wang R, Xiang L, Zhou H, Gu H. Identification of a subpopulation of long-term tumor-initiating cells in colon cancer. *Biosci Rep* 2020; **40** [PMID: 32729895 DOI: 10.1042/BSR20200437]
- 39 **Okita K**, Ichisaka T, Yamanaka S. Generation of germline-competent induced pluripotent stem cells. *Nature* 2007; **448**: 313-317 [PMID: 17554338 DOI: 10.1038/nature05934]
- 40 **Ordóñez-Morán P**, Dafflon C, Imajo M, Nishida E, Huelsen J. HOXA5 Counteracts Stem Cell Traits by Inhibiting Wnt Signaling in Colorectal Cancer. *Cancer Cell* 2015; **28**: 815-829 [PMID: 26678341 DOI: 10.1016/j.ccell.2015.11.001]
- 41 **Westhovens R**. Clinical efficacy of new JAK inhibitors under development. Just more of the same? *Rheumatology (Oxford)* 2019; **58**: i27-i33 [PMID: 30806706 DOI: 10.1093/rheumatology/key256]
- 42 **Genovese MC**, van Vollenhoven RF, Pacheco-Tena C, Zhang Y, Kinnman N. VX-509 (Decernotinib), an Oral Selective JAK-3 Inhibitor, in Combination With Methotrexate in Patients With Rheumatoid Arthritis. *Arthritis Rheumatol* 2016; **68**: 46-55 [PMID: 26473751 DOI: 10.1002/art.39473]
- 43 **Zhang N**, Ng AS, Cai S, Li Q, Yang L, Kerr D. Novel therapeutic strategies: targeting epithelial-mesenchymal transition in colorectal cancer. *Lancet Oncol* 2021; **22**: e358-e368 [PMID: 34339656 DOI: 10.1016/S1470-2045(21)00343-0]
- 44 **Eguchi T**, Csizmadia E, Kawai H, Sheta M, Yoshida K, Prince TL, Wegiel B, Calderwood SK. SCAND1 Reverses Epithelial-to-Mesenchymal Transition (EMT) and Suppresses Prostate Cancer Growth and Migration. *Cells* 2022; **11** [PMID: 36552758 DOI: 10.3390/cells11243993]
- 45 **Pastushenko I**, Blanpain C. EMT Transition States during Tumor Progression and Metastasis. *Trends Cell Biol* 2019; **29**: 212-226 [PMID: 30594349 DOI: 10.1016/j.tcb.2018.12.001]
- 46 **Lambert AW**, Weinberg RA. Linking EMT programmes to normal and neoplastic epithelial stem cells. *Nat Rev Cancer* 2021; **21**: 325-338 [PMID: 33547455 DOI: 10.1038/s41568-021-00332-6]
- 47 **Montague TG**, Gagnon JA, Schier AF. Conserved regulation of Nodal-mediated left-right patterning in zebrafish and mouse. *Development* 2018; **145** [PMID: 30446628 DOI: 10.1242/dev.171090]
- 48 **Hayes K**, Kim YK, Pera MF. A case for revisiting Nodal signaling in human pluripotent stem cells. *Stem Cells* 2021; **39**: 1137-1144 [PMID: 33932319 DOI: 10.1002/stem.3383]

- 49 **Kato Y**, Habas R, Katsuyama Y, Näär AM, He X. A component of the ARC/Mediator complex required for TGF beta/Nodal signalling. *Nature* 2002; **418**: 641-646 [PMID: [12167862](#) DOI: [10.1038/nature00969](#)]
- 50 **Duan W**, Li R, Ma J, Lei J, Xu Q, Jiang Z, Nan L, Li X, Wang Z, Huo X, Han L, Wu Z, Wu E, Ma Q. Overexpression of Nodal induces a metastatic phenotype in pancreatic cancer cells *via* the Smad2/3 pathway. *Oncotarget* 2015; **6**: 1490-1506 [PMID: [25557170](#) DOI: [10.18632/oncotarget.2686](#)]



Published by **Baishideng Publishing Group Inc**
7041 Koll Center Parkway, Suite 160, Pleasanton, CA 94566, USA
Telephone: +1-925-3991568
E-mail: office@baishideng.com
Help Desk: <https://www.f6publishing.com/helpdesk>
<https://www.wjgnet.com>

